NON FROPRIETARY VERSION

FRACTURE TOUGHNESS EVALUATION OF THE SHELL SIDE OF THE LOW PRESSURE COOLANT INJECTION SYSTEM (LPCI) HEAT EXCHANGER FOR DRESDEN STATION - UNIT 2

FRACTURE TOUGHNESS EVALUATION OF THE SHELL SIDE OF THE LOW PRESSURE COOLANT INJECTION SYSTEM (LPCI) HEAT EXCHANGER FOR DRESDEN STATION - UNIT 2

Table of Contents

List of Appendices

FRACTURE TOUGHNESS EVALUATION OF THE SHELL SIDE OF THE LOW PRESSURE COOLANT INJECTION SYSTEM (LPCI) HEAT EXCHANGER FOR DRESDEN STATION - UNIT 2

1.0 INTRODUCTION

This report presents the results from the fracture toughness evaluation of the shell side of the Low Pressure Coolant Injection (LPCI) system heat exchanger (HX) for Dresden Station Unit 2. This evaluation was performed to resolve the remaining open item for Commonwealth Edison Company's (CECo) review of the Systematic Evaluation Program (SEP), Topic III-1, Classification of Structures, Components and Systems which is to demonstrate that the shell sides of the LPCI-HXs have adequate fracture toughness. In NUREG-0577 , the USNRC calculates an average nil ductility temperature (NDT) of 40°F for plain carbon or mild steels, a group that includes A-212B, the LPCI-HX shell material. From this, the USNRC has concluded that material in this group will have adequate fracture toughness if its temperature is maintained above 77°F. A review of the LPCI system showed that the temperature of the LPCI-HX shell will be the same as the torus temperature. The torus temperature, as determined by a recorder chart from February 1989 dropped as low as 51°F . Since this is less than 77°F, CECo needed to determine whether the shell material has adequate fracture toughness at this temperature. The task of resolving this issue was assigned to by CECo as a request to perform a fracture toughness analysis of the LPCI-HX's shell side.

To perform the analysis, computer assisted calculations including 2-D and 3-D finite element analyses as well as hand calculations are employed. They are utilized in compliance with NUREG-0577 and with the ASME Boiler and Pressure Vessel Code, Section III Class C . The 2-D finite element analysis presented in Section 5.0 of this report is an overall axisymmetric analysis of the shell, tubesheet, tube bundle and head.

Its purpose is to simulate the effects from the interaction between sections of the HX (i.e., tube/tubesheet/shell interactions) and to calculate the maximum stress in the tubesheet caused by the structural (mechanical) and thermal load conditions that the HX is subjected to. Displacements from the 2-D finite element model were then applied to the detailed 3-D finite element model at nodes which represent common locations in the two models. The 3-D quarter symmetry model includes structural discontinuities in the HX that could not be modeled in the 2-D axisymmetric model because of their lack of axisymmetry to the vessel. The discontinuities analyzed are the shell side outlet nozzle and the vertical support bracket. By applying the displacements from the 2-D model to the locations common in the 3-D model and subjecting the 3-D model to the same loading conditions that are applied to the 2-D model, the maximum principal stress in the shell is calculated. This principal stress is used along with the material toughness, K_{IC}, , to determine the critical crack size for failure to occur, A_{cr}. Using the maximum stress range and the crack growth rate equation , the number of cycles, N, required for various assumed initial crack sizes, A_i, to grow to the critical crack size, A_{cr}, is calculated. This provides the desired fracture toughness characteristics of the LPCI-HX's shell side material, A-212B.

2.0 SUMMARY OF RESULTS

The LPCI-HX was analyzed by cycling it between steady-state operation and shutdown (assuming no flow and a worse case service temperature of 51°F throughout the vessel). The results from this analysis show that based upon an initial crack size of 0.010 inch (chosen as the maximum crack size that could go undetected by inspection of the unit at the time of construction) and a cold shutdown temperature of 51°F, the number of cycles (one cycle defined as steady-state operation to shutdown) that would be required to propagate a crack of this size to the critical crack size of 5.25 inches is

approximately 1.5 x 10^6. Based solely from this fracture mechanics analysis and a system startup and shutdown cycle occurring on an average of once a month, the acceptable number of cycles is far beyond any anticipated service life of the LPCI-HX as well as several orders of magnitude beyond the maximum conceivable plant lifetime including life extension. Therefore, the fracture toughness of the shell side of the LPCI-HX is more than adequate.

3.0 GENERAL DESCRIPTION

3.1 LPCI-HX Design

The Low Pressure Coolant Injection (LPCI) system heat exchanger is a two tube pass, split flow, shell-and-tube heat exchanger with the top stationary head having its channel integral with the fixed top tubesheet and the pass partition and having a removable channel cover. The bottom stationary head has its channel integral with the fixed bottom tubesheet and also has a removable channel cover. See Figure 1. The LPCI-HX has an overall length of 28 feet, 2-5/8 inches and is mounted vertically via three support brackets. The cylindrical shell has a 61 inch I.D. and a 7/8 inch wall thickness.

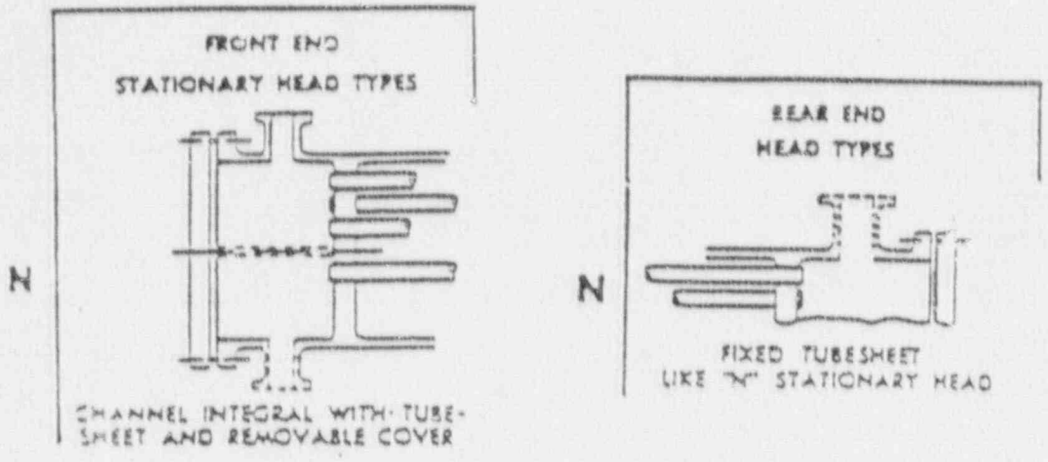

FIGURE 1 SHELL-AND-TUBE HEAD TYPES

The two tubesheets have a thickness of 3-3/4 inches each and are both overlayed with 1/4 inch monel clad steel. The tubesheets are welded to both the shell and the head. The unit has 2512 tubes on a 1.00 inch rotated square pitch. Each tube is 22 feet in length, has a 3/4 inch O.D. and an 18 BWG minimum wall thickness.

Each channel cover is attached using 60 - 1-3/8 inch bolts. The tube side inlet and outlet nozzles are 16 inch Schedule 40 pipe with a 1/2 inch wall thickness. The shell side inlet and outlet nozzles are 24 x 18 inch extra strong concentric reducers with a wall thickness of 1/2 inch throughout. Reinforcement pads, each having a 7/8 inch thickness, are welded to the nozzles for added support.

Details of the LPCI-HX are shown on the Heat Exchanger Specification Sheet and on the following PERFEX Corporation drawings:

Title	Drawing No.	Rev.
Outline Drawing (as built)	K-5009 - 1 & 2 Sheet 1	4
Outline Drawing (as built)	K-5009 - 1 & 2 Sheet 2	2
Orientation & Top Channel Assembly	4-5009-2	2
Shell & Bottom Channel Details and Assembly	4-5009-3	1
Tube Bundle Assembly & Details	4-5009-4	3
Gaskets	2-5004-1	0

3.2 LPCI-HX Materials

The LPCI-HX is constructed primarily of SA-212, Gr. B. Because of the discontinuance of A212 (identical with ASME Specification SA-212) in 1966 , the specification for High Tensile Strength Carbon Silicon Steel Plates for Boilers and Other Pressure Vessels was replaced by A515 (identical with ASME Specifications SA-515 specification for Carbon Steel Plates for Pressure Vessels for Intermediate and Higher

Temperature Service . Therefore, SA-212, Gr. B material properties are utilized when available; otherwise, SA-515, Gr. 70 material properties are used.

The cylindrical shell, tubesheets, heads, support brackets and reinforcement pads are constructed of SA-212, Gr. B. The tubes are constructed of AL-6XN, a superaustenitic stainless steel which has been developed by Allegheny Ludlum Corporation . Both tubesheets are layered with a monel steel cladding. The inlet and outlet nozzles on the shell side and tube side are constructed of SA-106, Gr. B, a carbon steel used for high temperature service. The bolts used to attach the two covers to their corresponding channels are constructed of SA-193, Gr. B7.

The material properties necessary for the analysis are as follows:

Material	Modulus of Elasticity (psi)	Density (lb/in^3)	Coefficient of Thermal Expansion (in./in./°F)	Thermal Conductivity (BTU/in.-s-°F)
SA-212, Gr. B (SA-515, Gr. 70)	28.8×10^6	0.283	5.76×10^{-6}	5.62×10^{-4}
AL-6XN	27.0×10^6	0.291	8.50×10^{-6}	1.83×10^{-4}
Monel 400 (67 Ni - 30 Cu)	26.0×10^6	0.319	7.74×10^{-6}	4.44×10^{-4}
SA-106, Gr. B	29.0×10^6	0.283	6.31×10^{-6}	6.82×10^{-4}
SA-193, Gr. B7 (1 Cr - 1/5 Mo)	29.2×10^6	0.283	6.31×10^{-6}	5.56×10^{-4}

All material properties are taken from unless otherwise stated. Material properties are evaluated at 165°F, the maximum shell side operating temperature . AL-6XN material properties, which are unavailable at this temperature, are evaluated at the ambient temperature of 70°F.

4.0 ANALYTICAL METHODS

The LPCI-HX is analyzed by a combination of hand calculations and detailed finite element analyses. The following is a list of computer programs used in the analyses:

Computer Program Information Forms are given on the pages that follow.

COMPUTER PROGRAM INFORMATION FORM

COMPUTER PROGRAM INFORMATION FORM (Con't)

COMPUTER PROGRAM INFORMATION FORM (Con't)

COMPUTER PROGRAM INFORMATION FORM (Con't)

COMPUTER PROGRAM INFORMATION FORM (Con't)

COMPUTER PROGRAM INFORMATION FORM (Con't)

5.0 OVERALL AXISYMMETRIC ANALYSIS OF SHELL, TUBESHEET, TUBE BUNDLE AND HEAD

5.1 Development of the Axisymmetric Finite Element Model

A two-dimensional axisymmetric finite element model of the heat exchanger is shown in Figures 5.1 to 5.5. This model, hereafter referred to as the tubesheet model, includes the tubesheet, the head, one-half of the shell barrel, the tubes, the monel layer on the tubesheet, and the closure studs. Since much similarity exits between K-5009-1 and K-5009-2, the two types of containment exchanger units (PERFEX Drawing Numbers K-5009-1 and 2 Sheet 1), heat exchanger K-5009-1 is chosen to be representative of the LPCI-HX for the analyses. The top half of the HX is analyzed because it contains discontinuities (shell side outlet nozzle, vertical support brackets, tubesheet to shell interface and tube side inlet and outlet nozzles) that are not all present in the lower half of the HX. Analyses that are performed using this model include structural (mechanical) and thermal load conditions that the heat exchanger is subjected to. The purpose of the tubesheet model is to apply these conditions to the overall heat exchanger in order to obtain the simulated effects from the interaction between sections of the HX (i.e., tube/tubesheet/shell interaction) and to determine the tubesheet stresses. The nozzles and the vertical support brackets are not included in the tubesheet model since they cannot be axisymmetrically represented in the model. Instead, these regions are analyzed using a 3-D finite element model described later in this report. Displacements from the 2-D model are applied to the 3-D finite element model in order to simulate the overall heat exchanger conditions at the nozzle and vertical support bracket discontinuities of the HX.

The LPCI-HX is a two-tube pass, split flow, shell-and-tube heat exchanger with a pass partition to separate flow in the top head. The pass partition could not be modeled in the tubesheet model because of its lack of axisymmetry. To show that its exclusion from the analysis would add

conservatism to the stresses in the tubesheet, two 3-D quarter symmetry models are used. The first model consists of the tubesheet with the attached partition plate and the second model consists of the tubesheet alone. A shell side pressure of 100 psi (an arbitrary value used for comparison purposes only) is applied to both models. The stresses in the tubesheet without the partition plate are approximately two times those in the model with the partition plate. See Figures 5.7 to 5.13. In addition, the exclusion of the partition plate would induce greater rotations into the shell which is also conservative. Therefore, it is concluded that by not including the partition plate in the analysis the stresses that would occur in the tubesheet and shell would be higher than those in reality. This is a conservative approach in the analysis.

The tubesheet model and the two 3-D quarter symmetry models used in the aforementioned evaluation are analyzed using the a computer program . The two 3-D models are made with elastic quadrilateral shell elements . In the tubesheet model, the tubesheet, shell barrel, monel layer and head are represented by 2-D isoparametric solid elements . The tubes and closure stud elements are modeled using 2-D elastic beams .

General material properties for the components included in the tubesheet model are given in Section 3.2 of this report. The maximum range of temperature which the LPCI-HX is subjected to is 51°F-165°F. Where 51°F is the assumed lowest HX temperature since a temperature as low as 51°F was recorded in February 1989 and 165°F is the maximum shell side inlet temperature . Since thermal stresses are proportional to the product of the modulus of elasticity, E, and the coefficient of thermal expansion, α, the temperature that maximizes the product $E\alpha$ is chosen. For this range of temperature, 165°F produces the maximum product of $E\alpha$, therefore, material properties are evaluated at 165°F. Since material properties for AL-6XN are unavailable at this

temperature, properties at ambient temperature (70°F) are used. Material properties utilized in the finite element analyses are summarized in Appendix A.1.

Two regions of the tubesheet model which require modifications of the material properties are the stud holes located in the channel flange and the channel cover. Modifications to the general material properties given in Section 3.2 are calculated in Appendix A.2. This set of adjusted properties is used for all load cases. The reduced stiffness in the annulus formed by the stud holes is accounted for by modifying the modulus of elasticity in the radial and axial directions by the ratio of the actual material in the annular stud hole region to the total material modeled in that same annular region. The circumferential modulus is set to 1.0 to simulate the lack of hoop stiffness in the hole region. The density of these regions is also modified by the area ratio described above.

The perforated tubesheets are modeled as equivalent solid plates following the guidelines outlined in Article A-8000 in Appendix A of the ASME Boiler and Pressure Vessel Code

The effective boundary of the equivalent material of the tubesheet, R*, is based upon the irregular outer boundary of the unit cells . The dimensions for this particular case are given in Appendix 3 of this report. The calculated value of R* is 28.28 inches.

The tubes are modeled as 2-D beams whose properties represent an axisymmetric equivalent to the sum of the actual tubes swept out by the annulus centered on the beam.

A summary of the properties for each beam in the model is given in Appendix A.3. Also included are the initial strains for the beam elements to simulate the elongation or contraction of

the tubes due to internal and external pressure. The pressure inside (tube side pressure) and outside (shell side pressure) the tubes cause the tubes to change length axially due to the Poisson ratio effect.

Constraint equations are used at the tube-tubesheet interfaces to provide "built in" conditions for the tubes. This is accomplished by forcing the rotation of each beam element at the tube-tubesheet interface nodes to be equal to the relative axial displacement of the two adjacent tubesheet nodes divided by the distance between the adjacent nodes (i.e., the beam element is forced to remain perpendicular to the tubesheet surface as the tubesheet rotates.)

The main closure studs joining the channel and the channel cover of the head are represented in the model by beam elements with "per radian" properties. Calculations for these properties are given in Appendix A.4 . Stud beam elements extend beyond the flange surface a distance equal to one-half of the stud diameter. This additional length accounts for the flexibility of the stud and fastener and is calculated . Rigid beam elements are used to connect the ends of the stud to the flanges via the node coupling scheme shown in Figure 5.2 and 5.3. By coupling the studs to the flanges in this manner, axial, radial and rotational displacements of the flanges are imposed upon the stud.

At the flange seating surface, compressive loads must exist during operation to prevent leaks. Therefore, in order to have a mathematically linear model and to simulate the gasket's performance during operational loads, two nodes at the gasket seating surface are coupled together axially (see Figure 5.4). This will be the only connection between the channel and channel cover besides the beams used to represent the studs. Stud preload can then be adjusted to ensure that tensile loads do not develop at the seating surface. This coupling method also allows the impact of the closure joint slipping from bolt preload to be

included since relative radial motion between the components is not restrained at the seating surface.

5.2 Base Case Loads

The tubesheet finite element model described in Section 5.1 is analyzed for various base case loadings. Stress and displacement results from these base cases are then combined to provide results for the required steady-state operation and shutdown conditions. The base case loads and a description of each are listed below. In all cases, the displacement boundary conditions specified are no axial motion at the axial symmetry plane of the shell barrel and tubes, no rotation at the axial symmetry plane of the tubes and no radial motion of the tubes at the baffle plate locations. Figure 5.6 is a node plot showing the boundary constraints described above.

Base Case 1: Preload on the Main Closure Studs

An initial strain of 0.0011 in./in. is applied to the beam elements representing the studs which join the channel cover to the channel flange to simulate a preload of 25,100 lb/bolt,
, in the beam elements. No other loads are applied.

Base Case 2: Tube Side Pressure = 185 psi

A pressure of 185 psi is applied to the inner surface of the head and to the non-perforated tube side surface of the tubesheet. For the perforated region the equivalent tube side pressure is 123.23 psi
. Included in the model is the initial strain on the tube beam elements to simulate growth due to internal tube pressure and a uniform tubesheet temperature of 185°F. The uniform temperature coupled with the modified value of ALPX simulates the effect of pressure in the perforations .

Base Case 3: Shell Side Pressure = 155 psi

A pressure of 155 psi is applied to the non-perforated, shell side surface of the tubesheet and to the inner surface of the shell. For the perforated region, the equivalent shell side pressure is 86.52 psi . The uniform tubesheet temperature is not required for this load case since there is no pressure in the penetrations. The initial strain to simulate tube growth due to external pressure is included .

Base Case 4: Steady-State Operating Temperatures

Temperatures are applied to the axisymmetric model as shown in Figures 5.14 and 5.15. The temperatures of 95°F on the tube side and 165°F on the shell side are conservatively chosen because of this being the maximum temperature extremes that the LPCI-HX is subjected to . The tube temperature, 122°F, is calculated . These temperatures are applied to the model to simulate thermal strains caused by expansion due to the temperature differences. The reference temperature is set to 70°F for the thermal strain calculations. Thermal strains are a function of the product of the coefficient of thermal expansion and the difference between the actual temperature and the reference temperature. No other loads are applied.

Base Case 5: No Flow Thermal Conditions (Shutdown)

To simulate shutdown thermal conditions, a uniform temperature of 51°F (the assumed worse case temperature, , that the entire vessel is subjected to) is applied throughout the vessel. The reference temperature is set to 70°F for thermal strain calculations. This temperature allows for any thermal contractions caused by a temperature drop below the reference temperature. No other loads are applied.

5.3 Operational Loads

Two operational load cases are analyzed by combining base case loads that are applicable during specific operating conditions. The base case loads are combined by using a computer program
Stresses and displacements from the individual base cases are mathematically combined in order to obtain the desired resulting operational load case. The operational load cases and a description of each are listed below.

Steady State Operation

Steady-state operation is a combination of the base case loads: preload, tube side pressure, shell side pressure and steady-state operating temperatures. This case simulates the LPCI-HX being at full steady-state operating conditions.

No Flow Condition (Shutdown)

Shutdown is a combination of the base case loads: preload and no flow thermal conditions. This case simulates the LPCI-HX being shutdown with the temperature of the vessel dropping to 51°F.

5.4 Axisymmetric Analysis Results

The maximum stress due to steady-state operation is 15,030 psi. This value, which is located in the tubesheet, is calculated
. Displacement plots for the two operational loads (steady-state and shutdown) are shown
. Radial and hoop stress contour plots are shown
, respectively.

Displacement conditions from the 2-D model are next applied to the 3-D model at common nodal locations in the two models, herein referred to as the cut boundaries, to simulate these conditions at the modeled discontinuities described in Section 6.0 of this report.

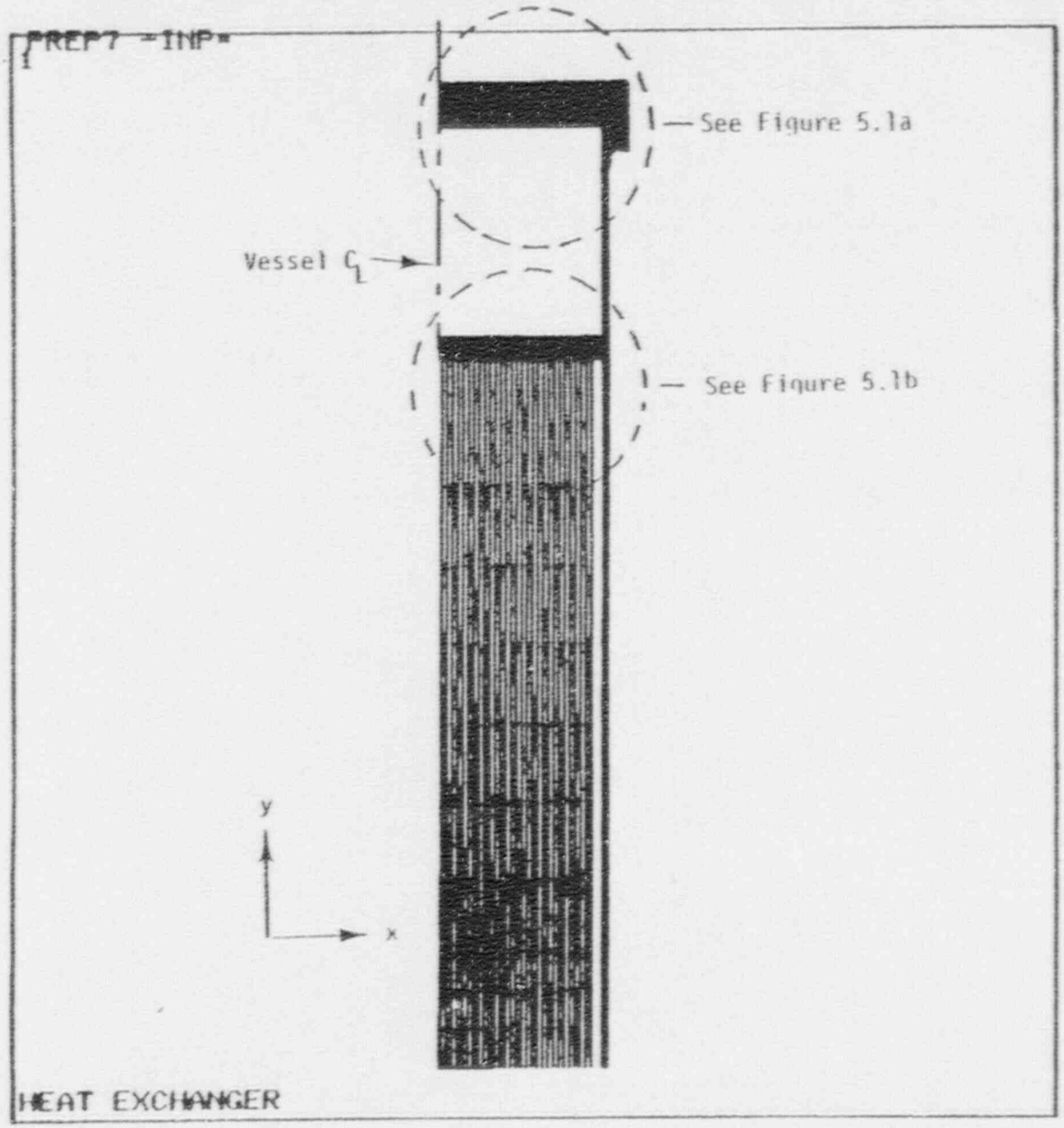

FIGURE 5.1 TUBESHEET FINITE ELEMENT MODEL GEOMETRY

NON PROPRIETARY VERSION

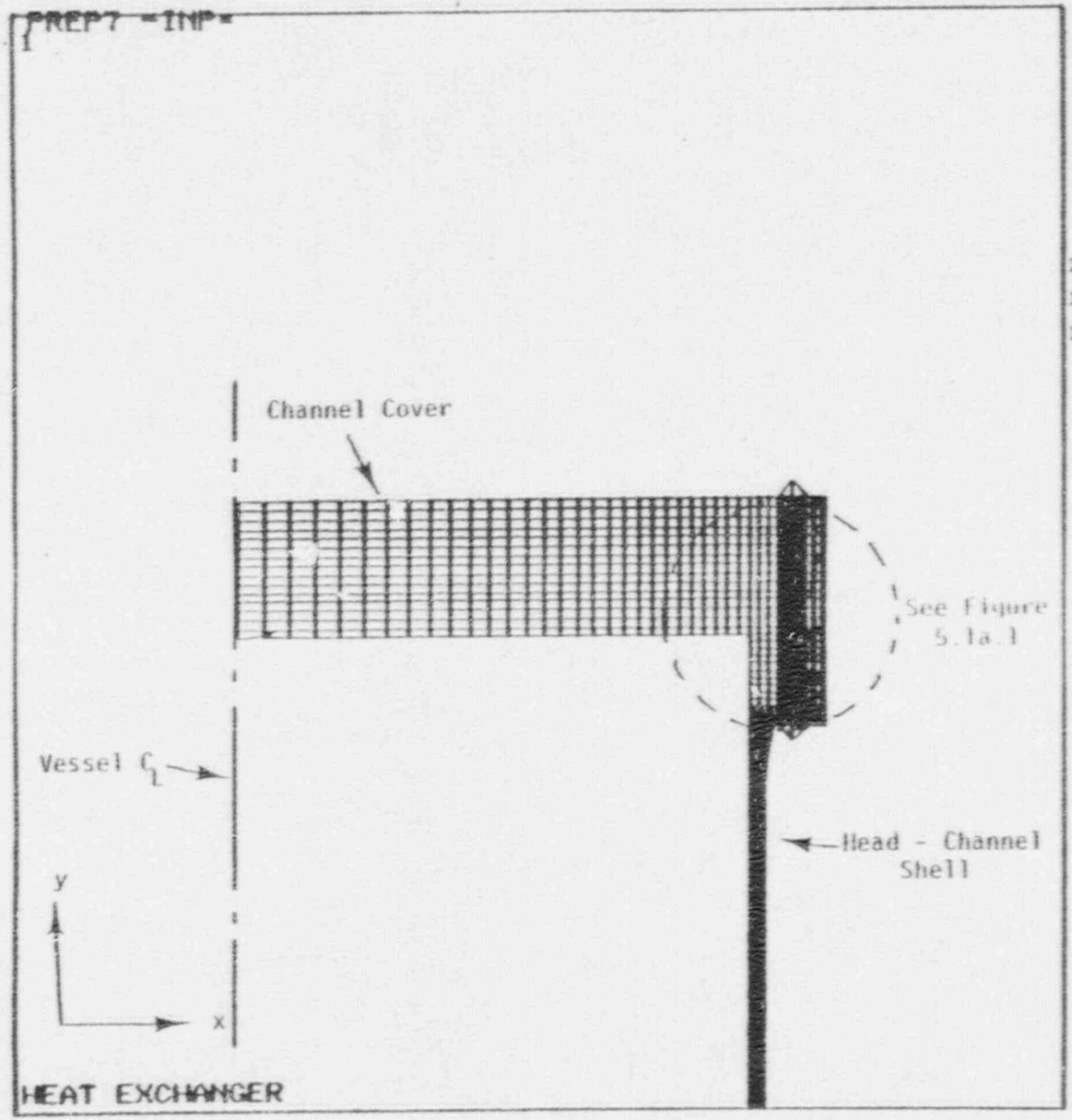

FIGURE 5.1a TUBESHEET FINITE ELEMENT MODEL GEOMETRY

2042.04-400-002-00 NON PROPRIETARY VERSION Page 24 of 61

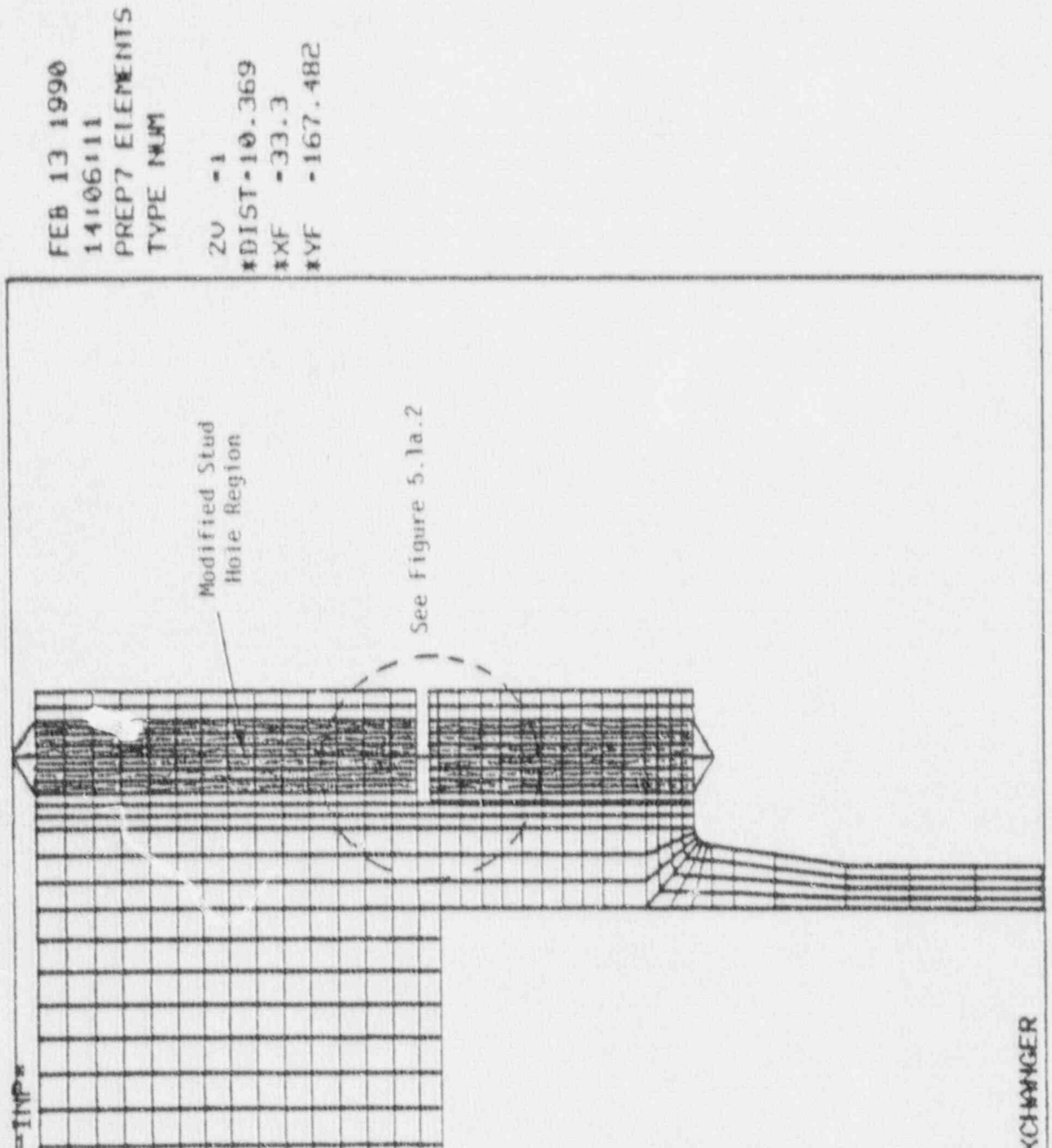

FIGURE 5.1a.1 TUBESHEET FINITE ELEMENT MODEL GEOMETRY

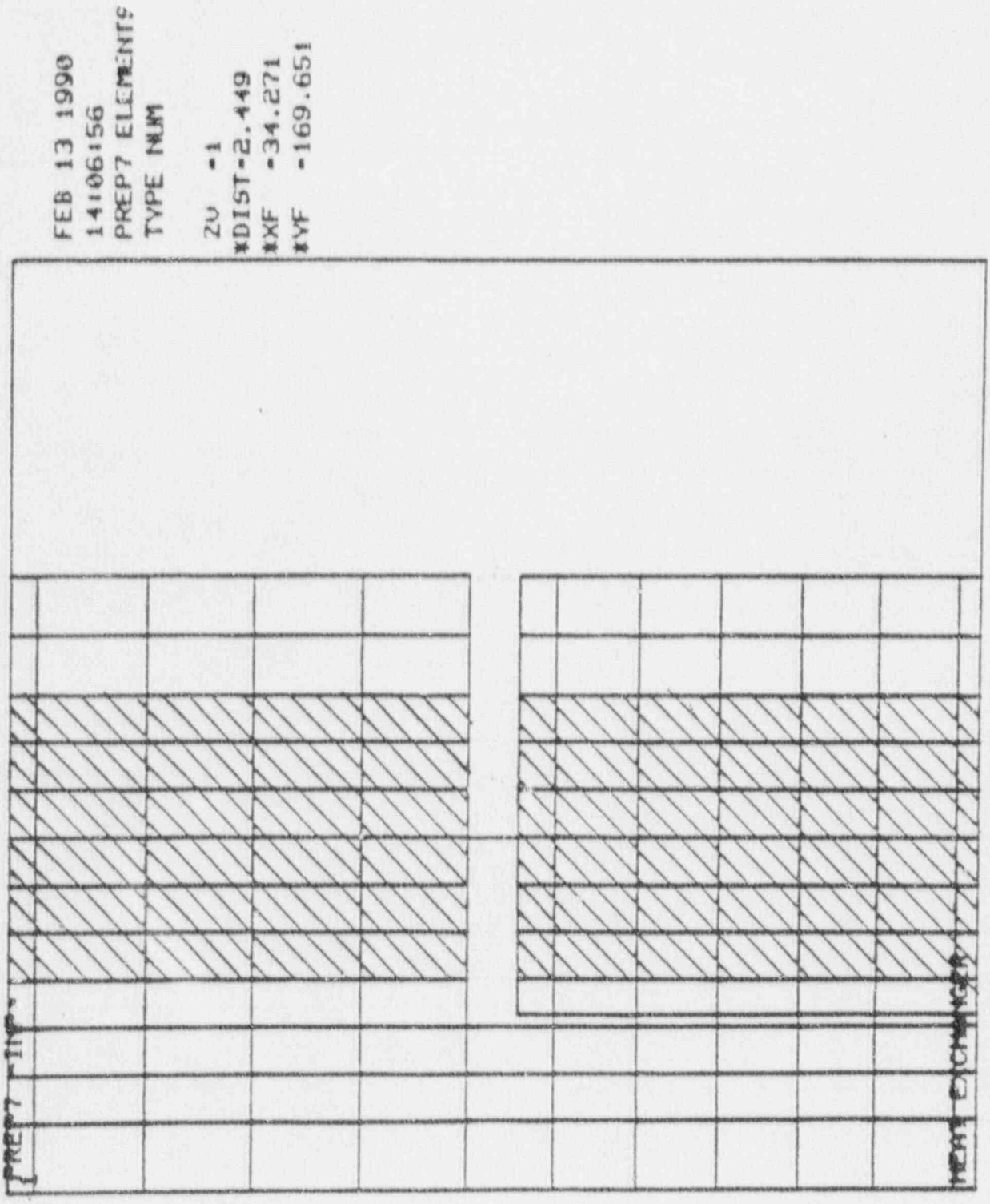

FIGURE 5.1a.2 TUBESHEET FINITE ELEMENT MODEL GEOMETRY

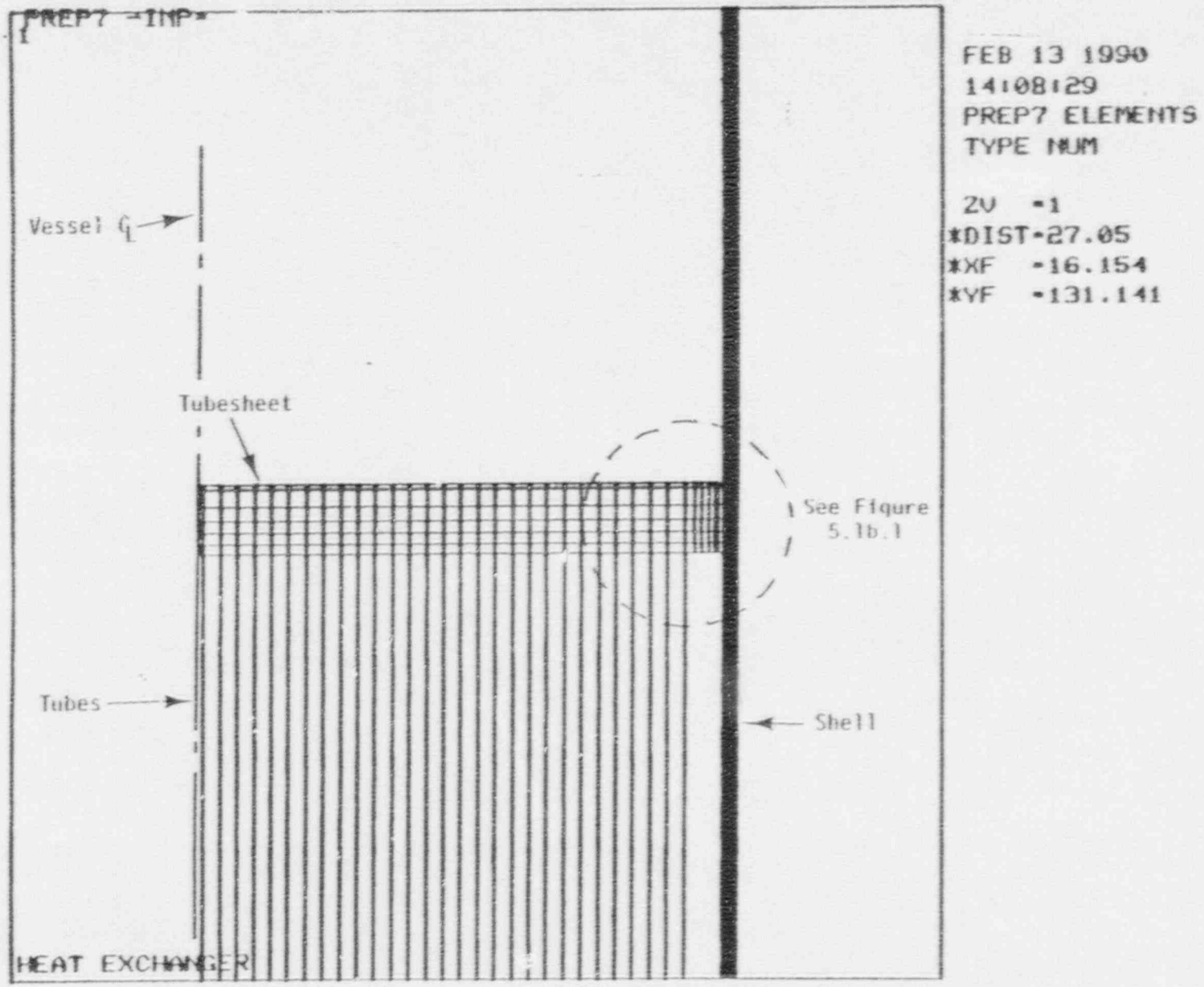

FIGURE 5.1b TUBESHEET FINITE ELEMENT MODEL GEOMETRY

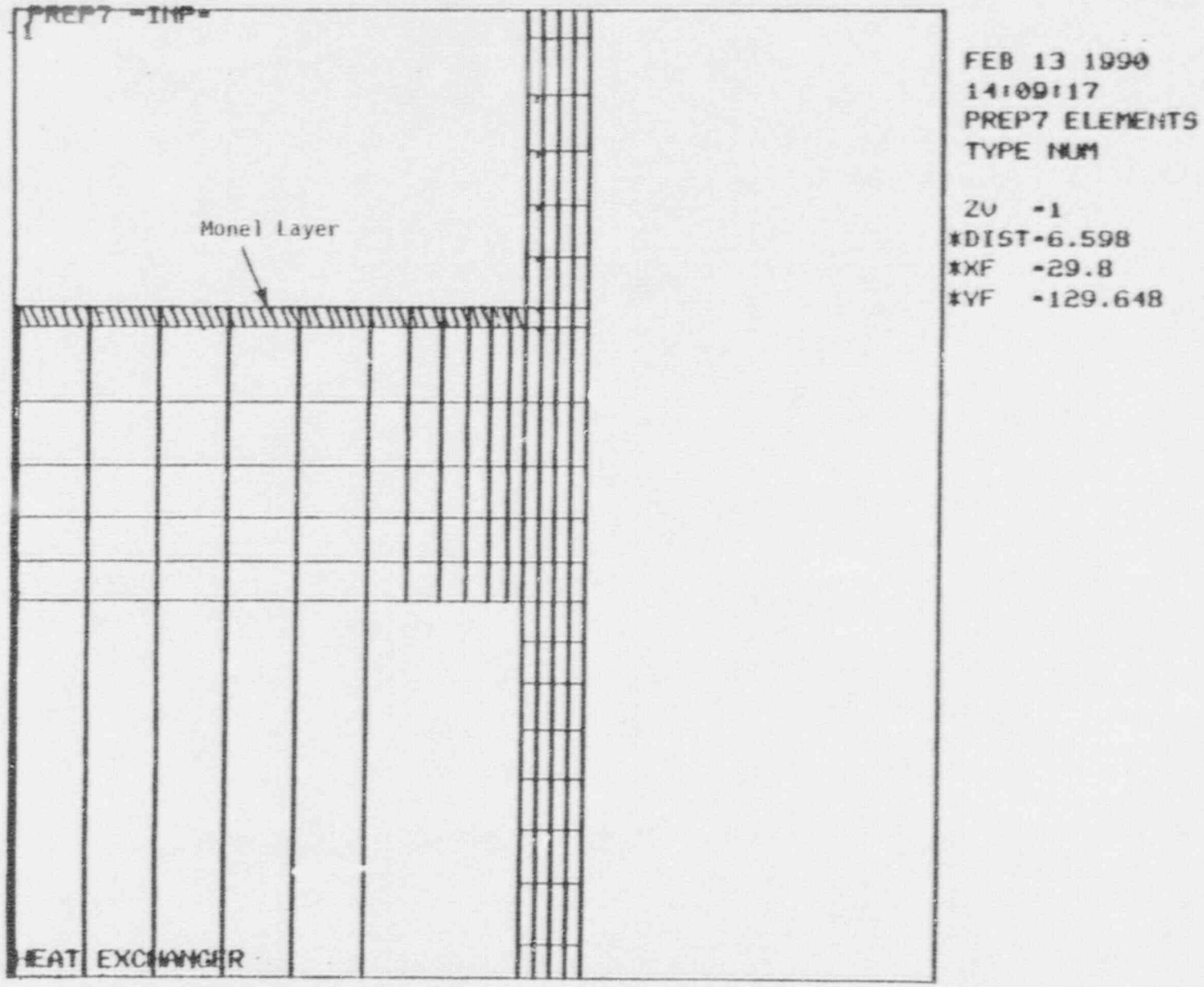

FIGURE 5.1b.1 TUBESHEET FINITE ELEMENT MODEL GEOMETRY

NON PROPRIETARY VERSION

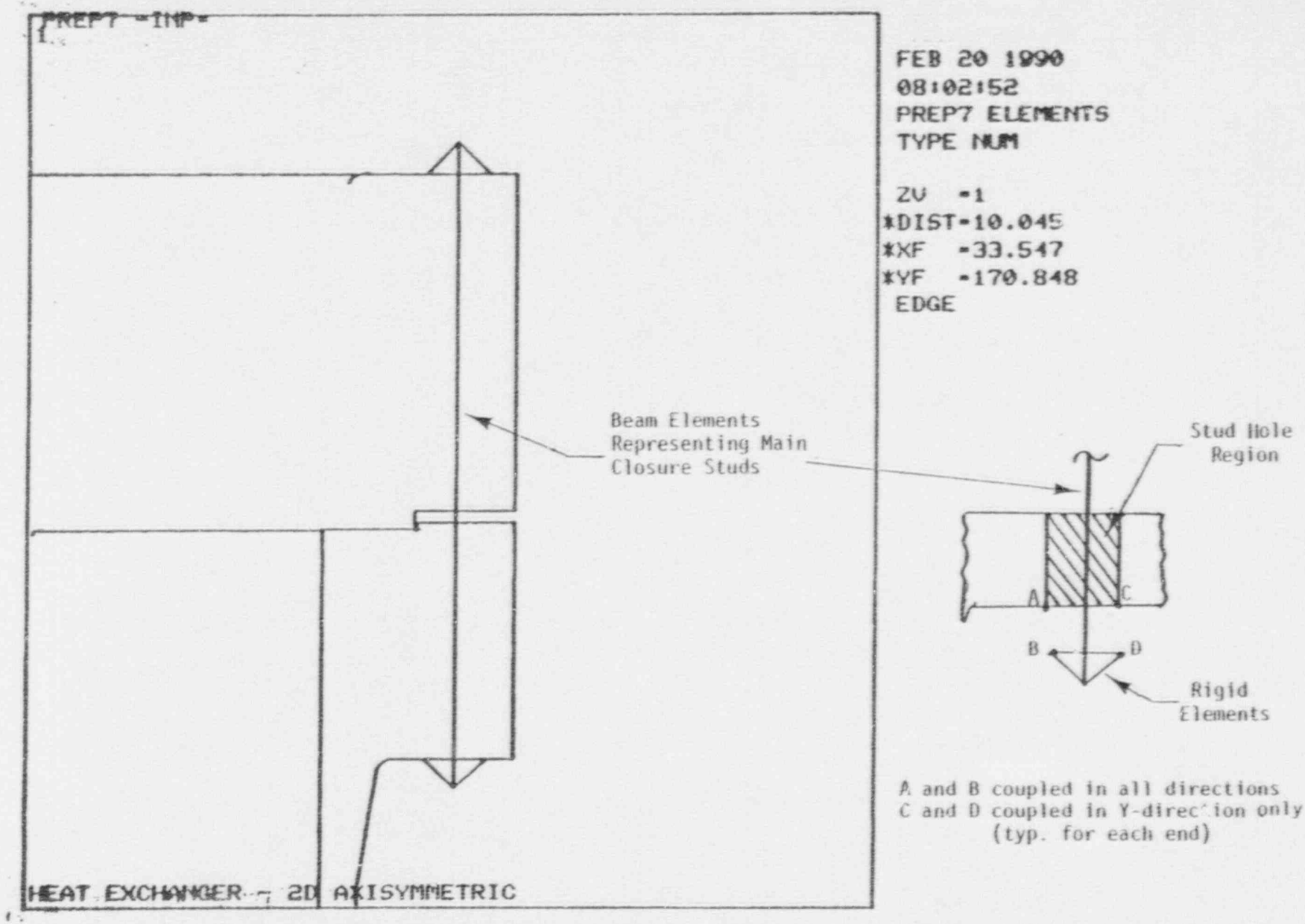

FIGURE 5.2 TUBESHEET FINITE ELEMENT MODEL GEOMETRY

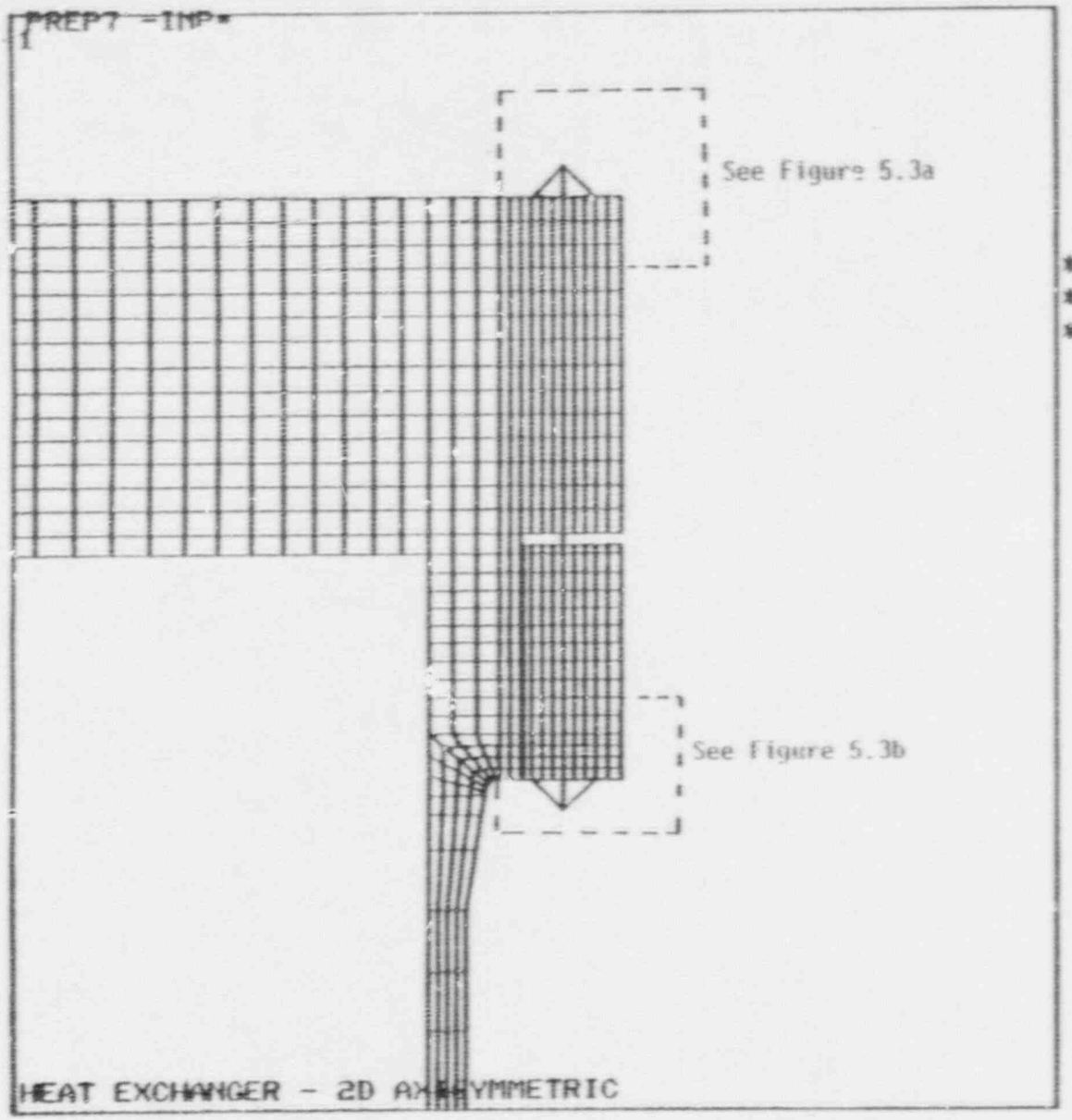

FIGURE 5.3 TUBESHEET FINITE ELEMENT MODEL GEOMETRY

NON PROPRIETARY VERSION

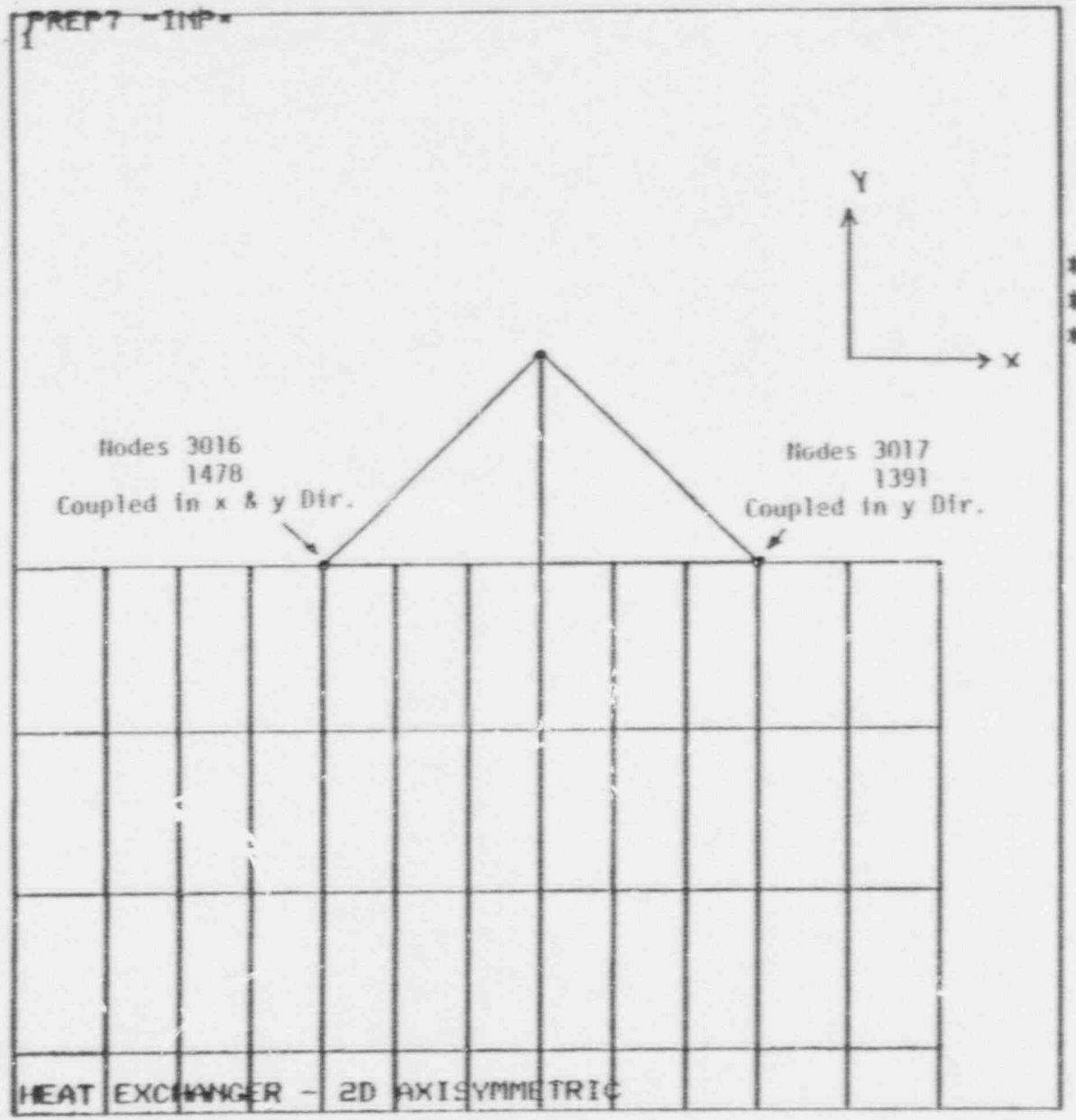

FIGURE 5.3a TUBESHEET FINITE ELEMENT MODEL GEOMETRY

NON PROPRIETARY VERSION

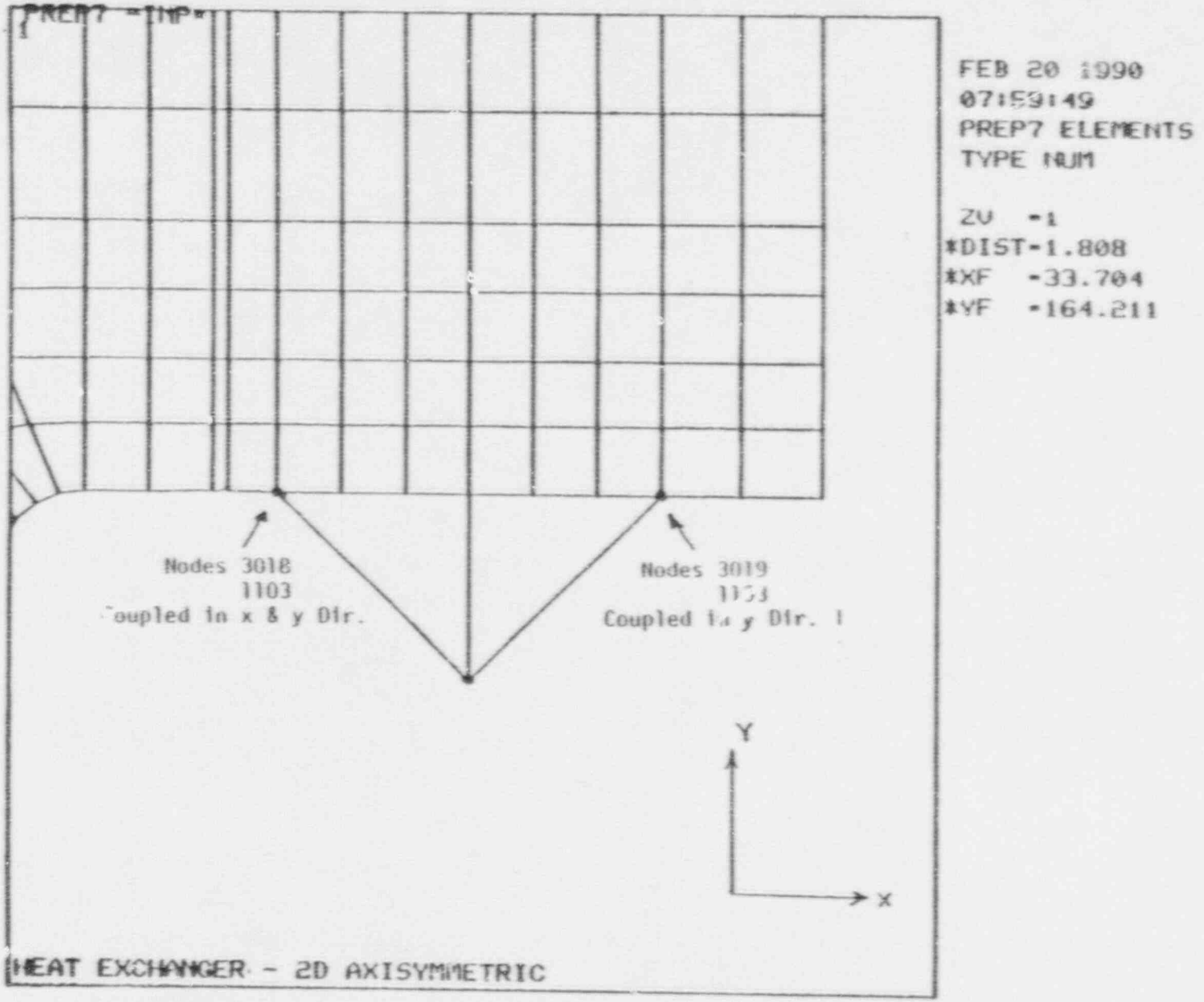

FIGURE 5.3b TUBESHEET FINITE ELEMENT MODEL GEOMETRY

NON PROPRIETARY VERSION

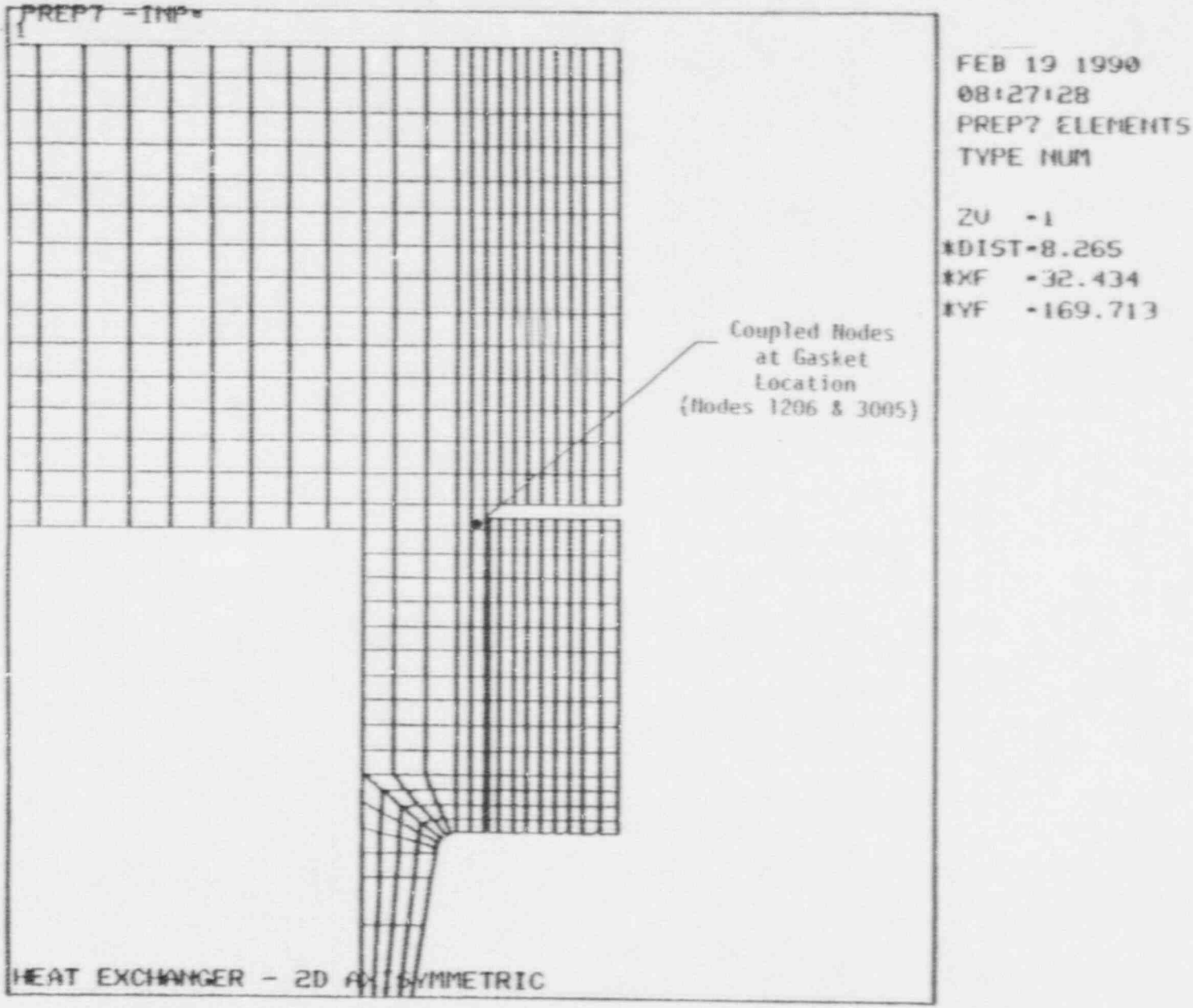

FIGURE 5.4 TUBESHEET FINITE ELEMENT MODEL GEOMETRY

NON PROPRIETARY VERSION

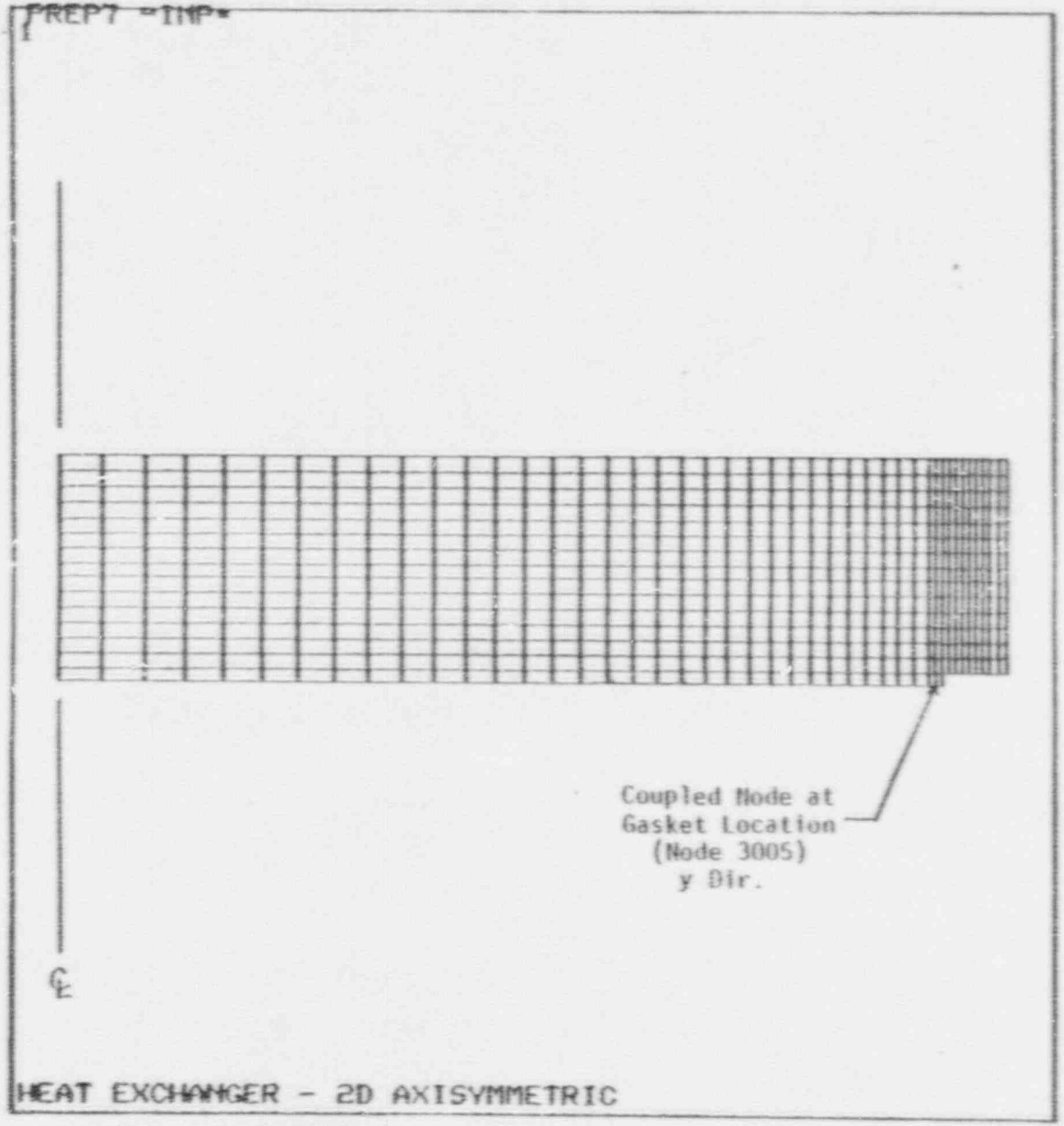

FIGURE 5.4a TUBESHEET FINITE ELEMENT MODEL GEOMETRY

NON PROPRIETARY VERSION

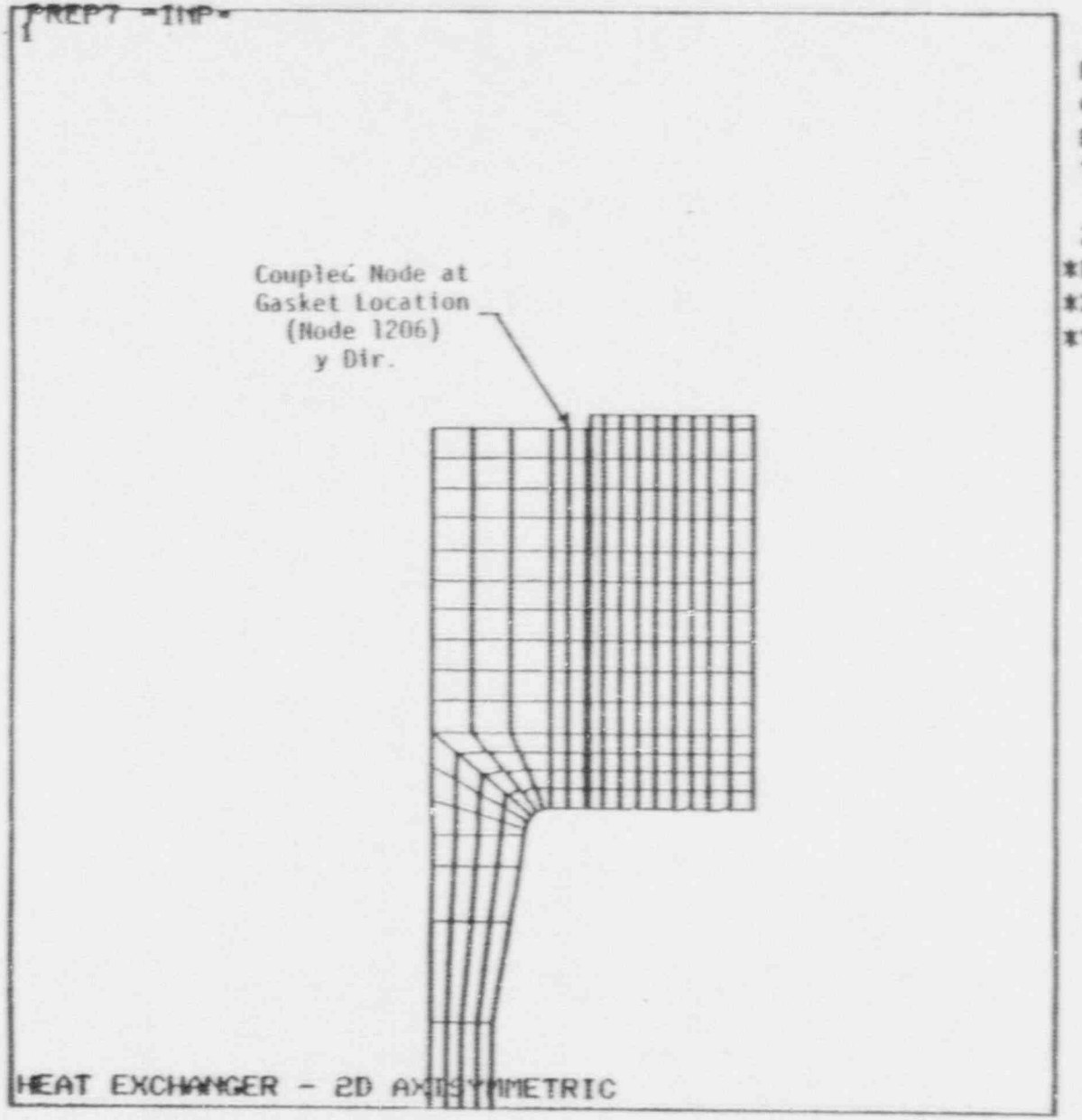

FIGURE 5.4b TUBESHEET FINITE ELEMENT MODEL GEOMETRY

NON PROPRIETARY VERSION

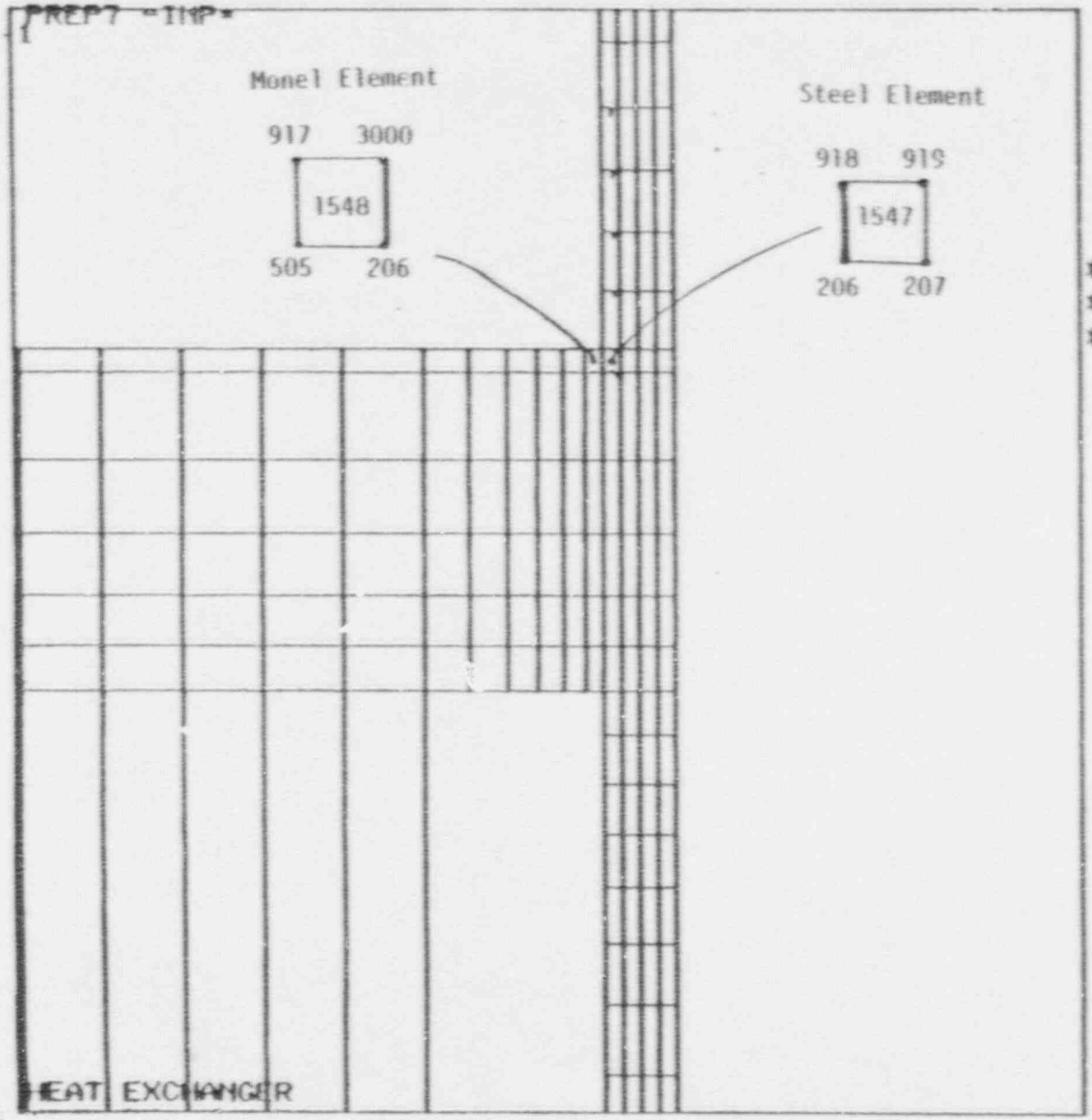

FIGURE 5.5 TUBESHEET FINITE ELEMENT MODEL GEOMETRY

NON PROPRIETARY VERSION

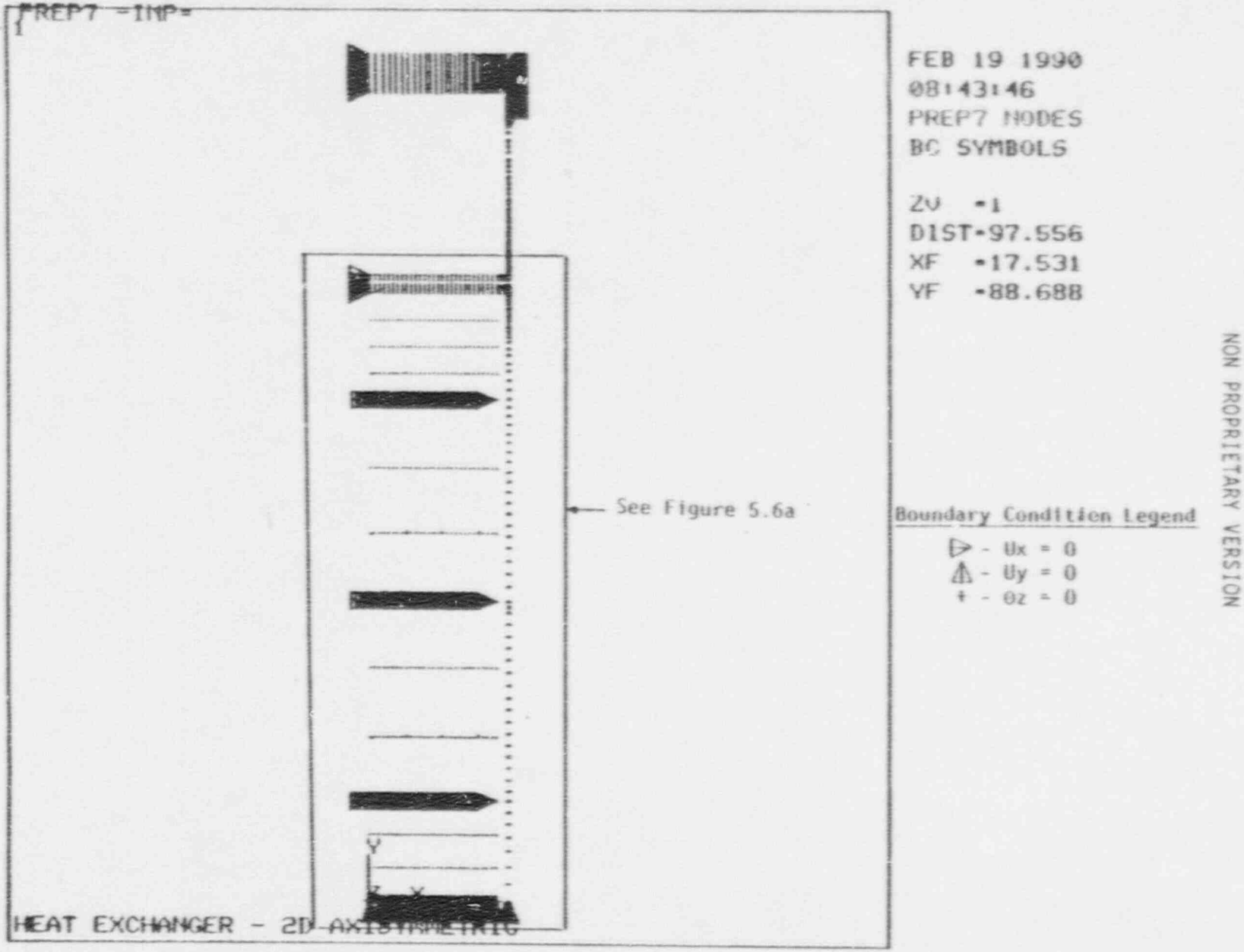

FIGURE 5.6 TUBESHEET FINITE ELEMENT MODEL DISPLACEMENT BOUNDARY CONDITIONS

NON PROPRIETARY VERSION

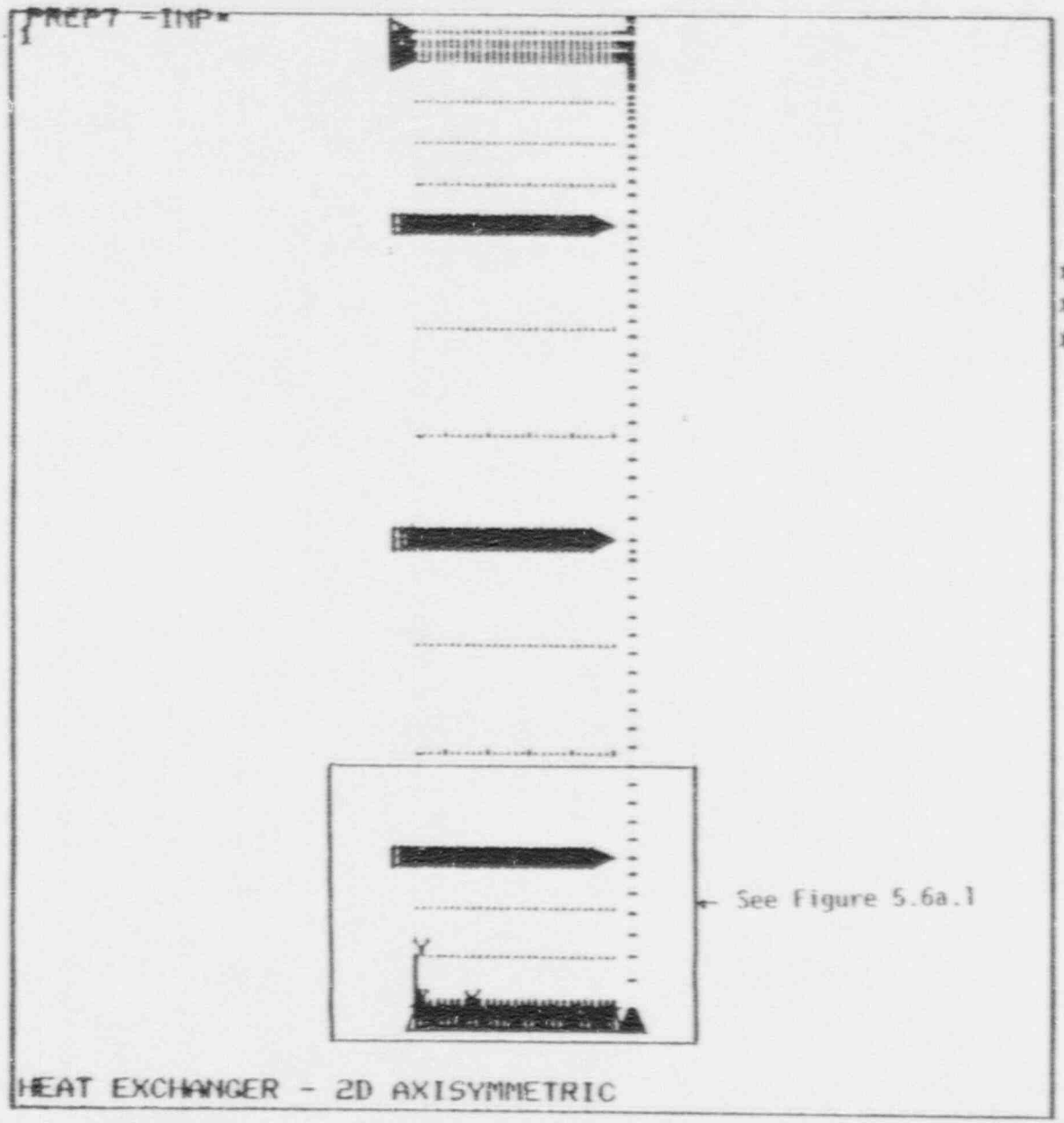

FIGURE 5.6a TUBESHEET FINITE ELEMENT MODEL DISPLACEMENT BOUNDARY CONDITIONS

NON PROPRIETARY VERSION

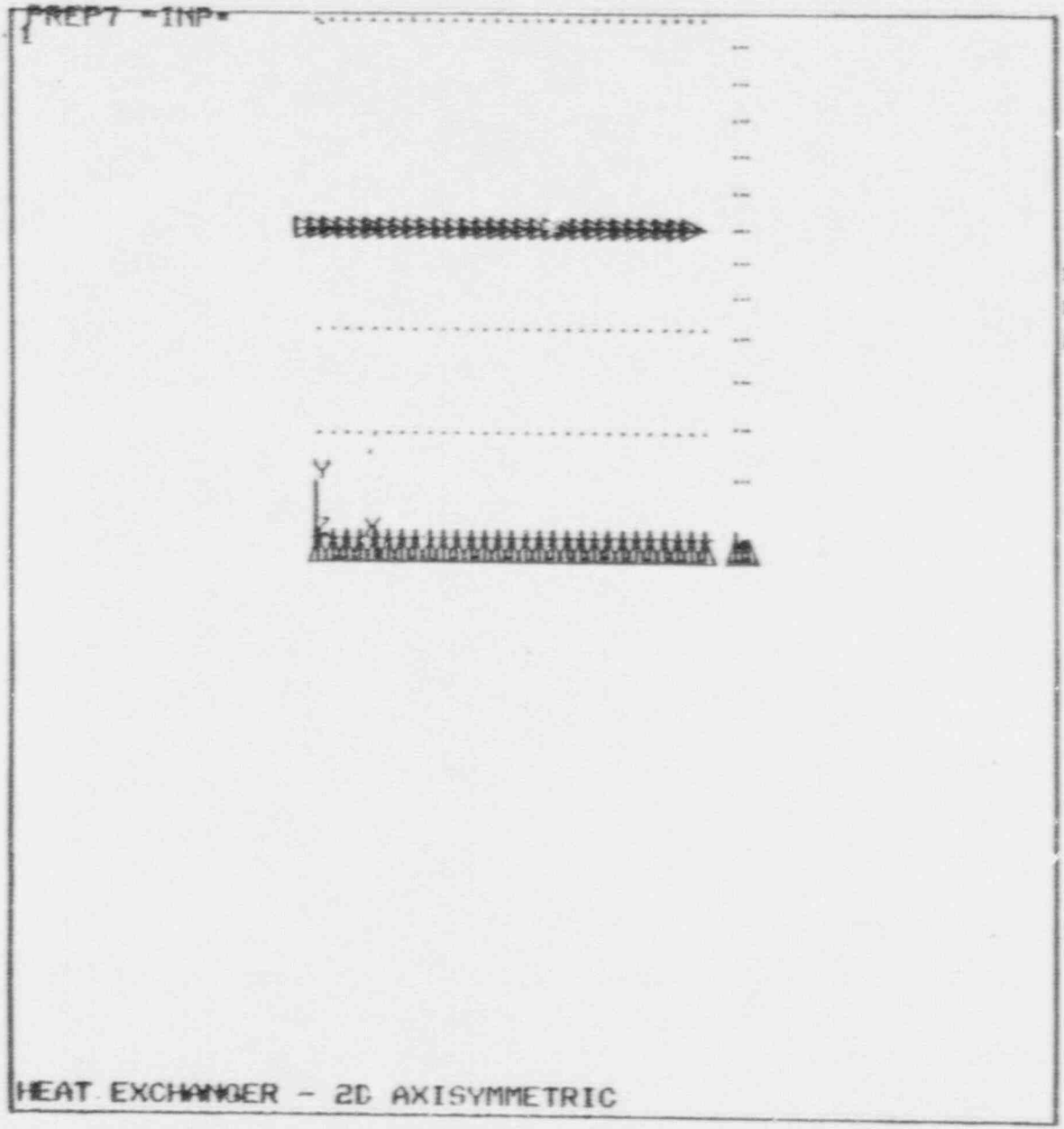

FIGURE 5.6a.1 TUBESHEET FINITE ELEMENT MODEL DISPLACEMENT BOUNDARY CONDITIONS

NON PROPRIETARY VERSION

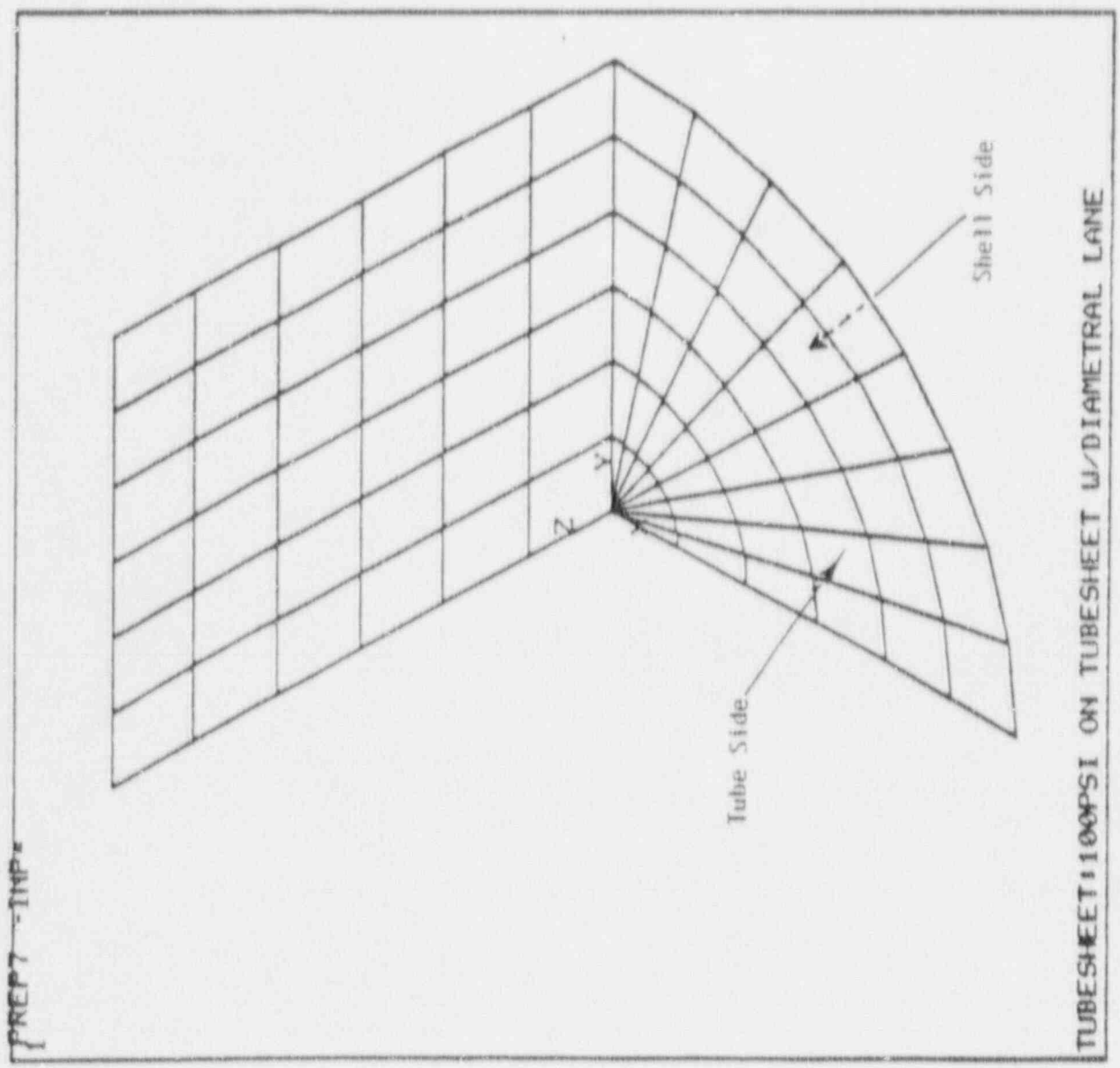

FIGURE 5.7 TUBESHEET WITH PARTITION PLATE (DIAMETRAL LANE) GEOMETRY

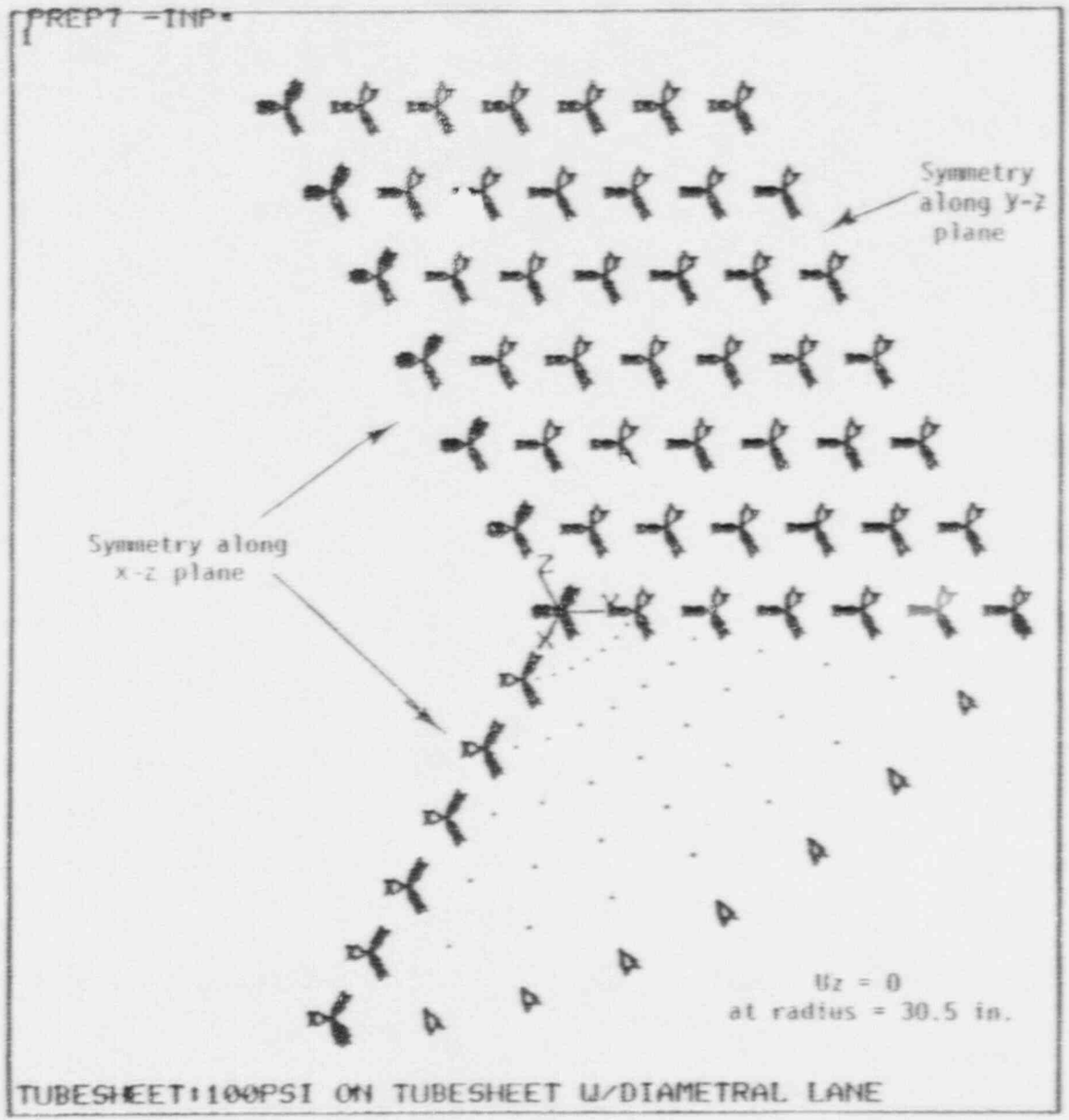

FIGURE 5.8 DISPLACEMENT BOUNDARY CONDITIONS

NON PROPRIETARY VERSION

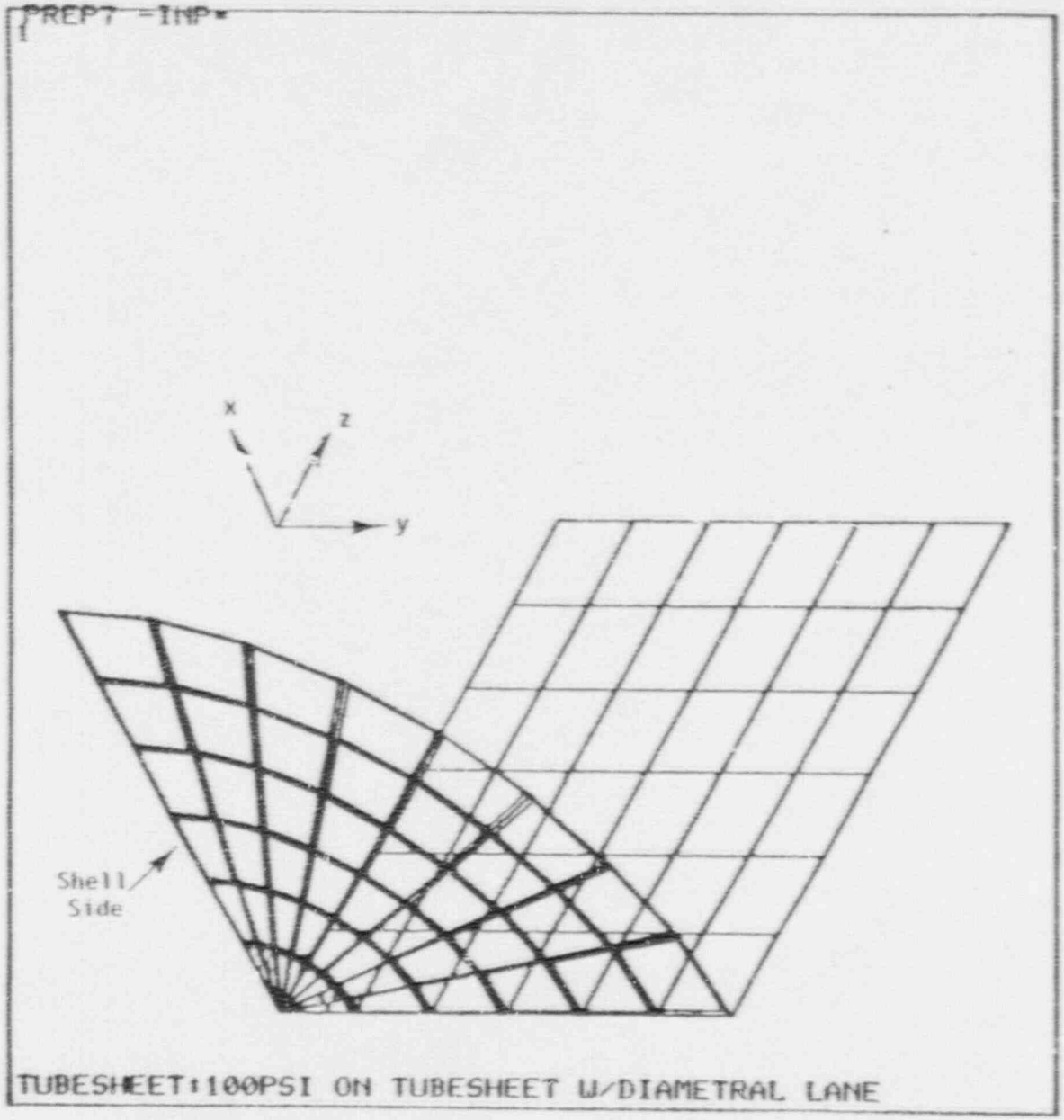

FIGURE 5.9 SHELL SIDE PRESSURE OF 100 PSI

NON PROPRIETARY VERSION

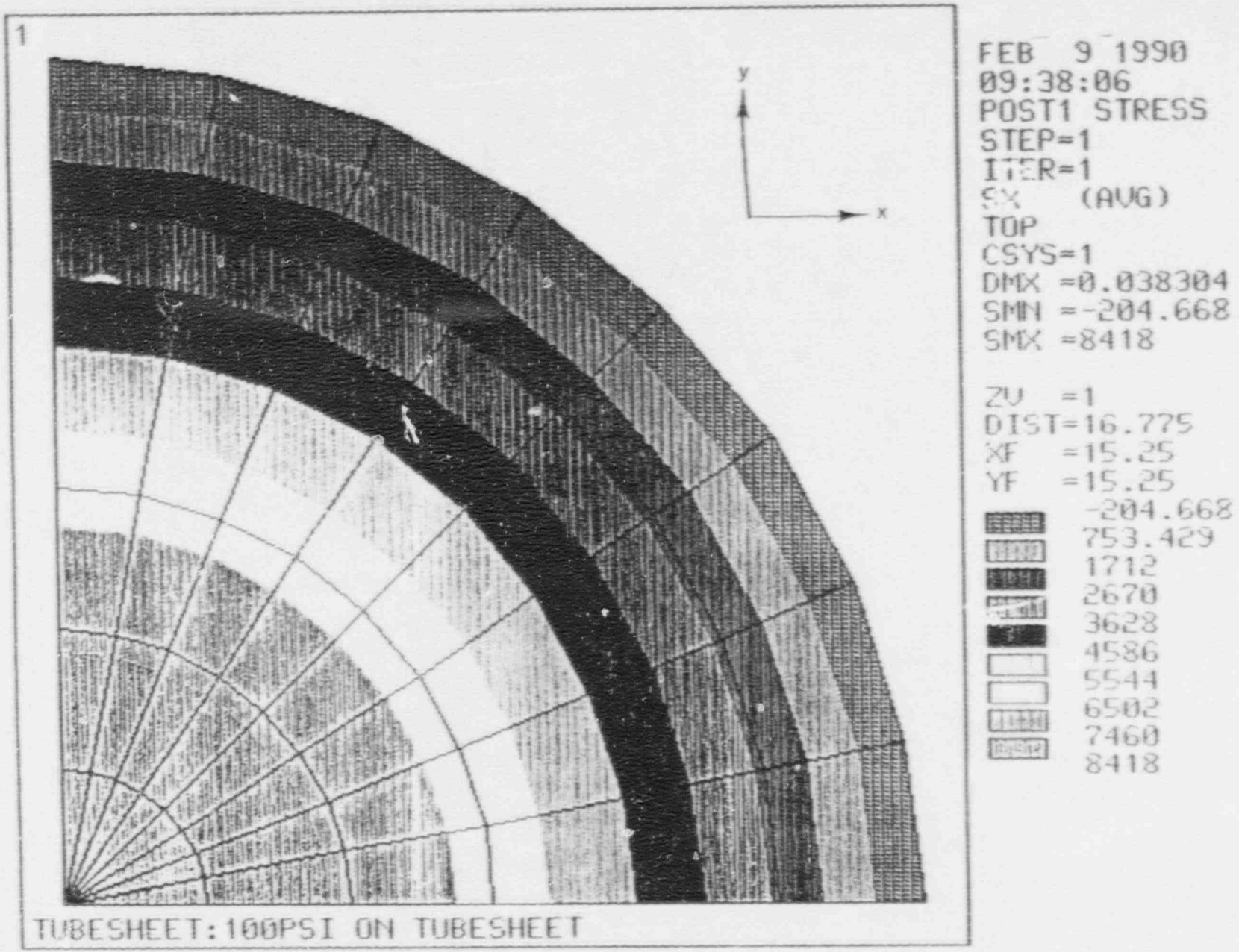

FIGURE 5.10 TUBESHEET WITHOUT PARTITION PLATE - RADIAL STRESS (S_x)

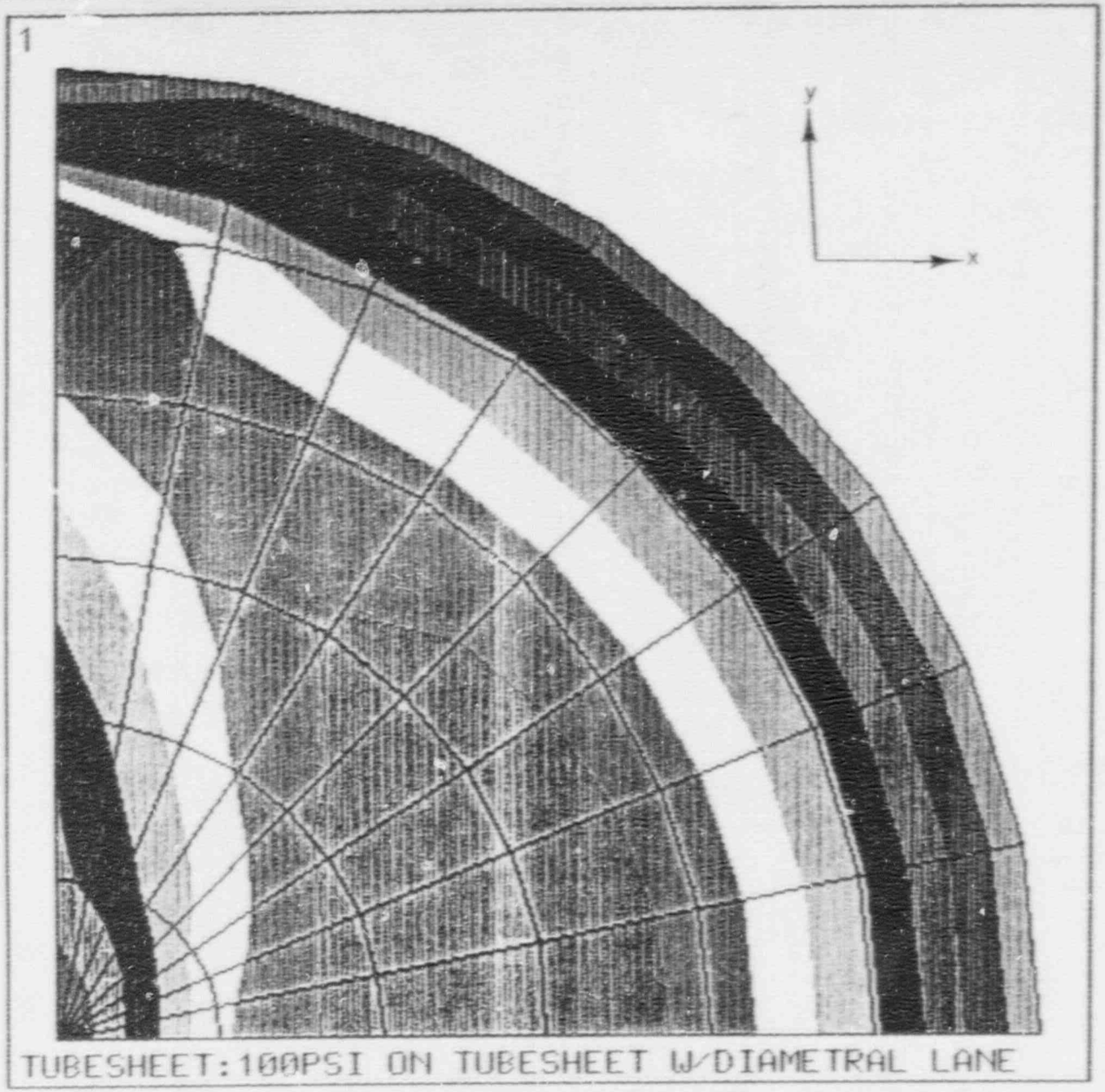

FEB 9 1990
09:32:49
POST1 STRESS
STEP=1
ITER=1
SX (AVG)
TOP
CSYS=1
DMX =0.015279
SMN =-665.147
SMX =3871

ZV =1
DIST=16.775
XF =15.25
YF =15.25

-665.147
-161.085
342.977
847.039
1351
1855
2359
2863
3367
3871

FIGURE 5.11 TUBESHEET WITH PARTITION PLATE - RADIAL STRESS (S_x)

NON PROPRIETARY VERSION

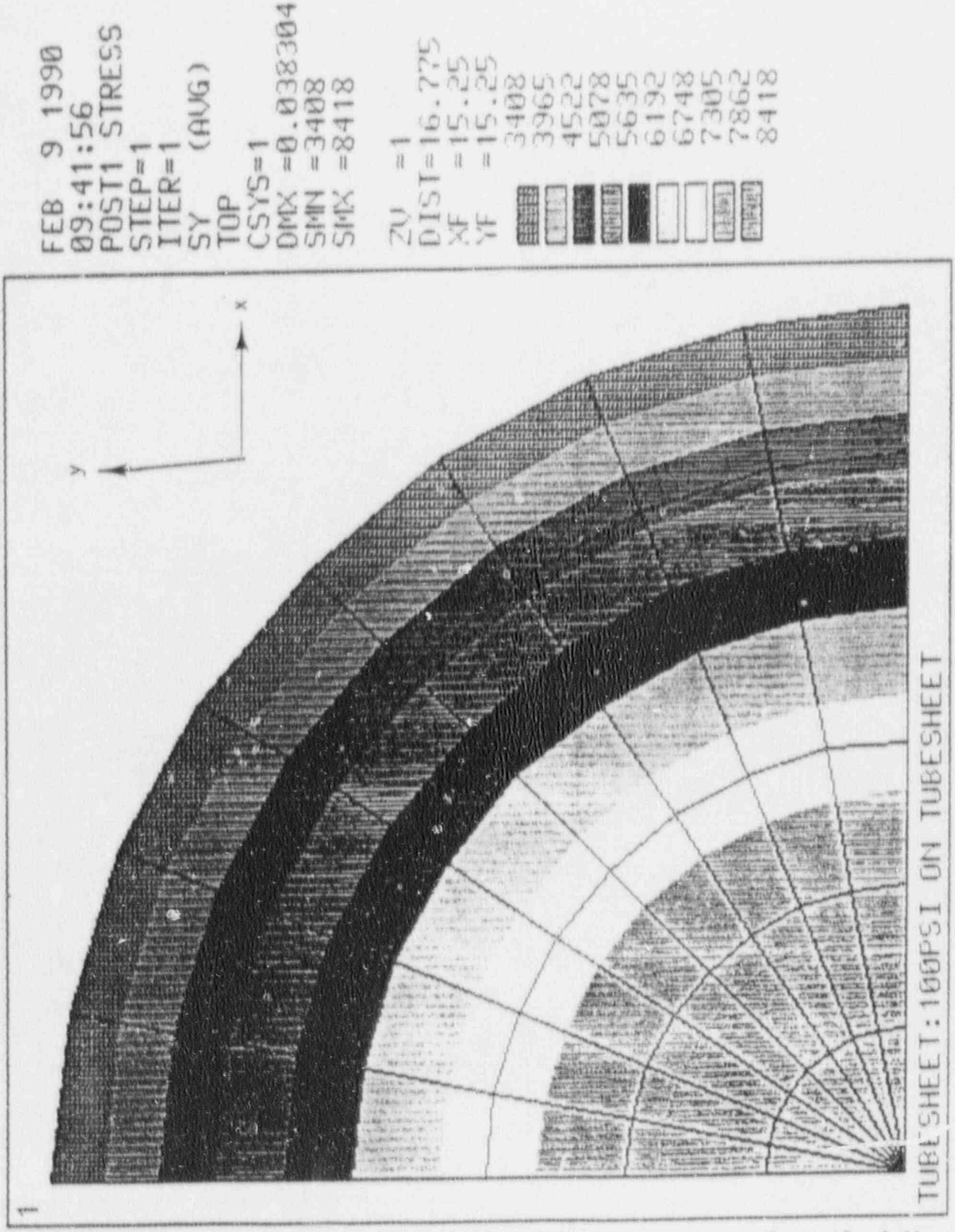

FIGURE 5.12 TUBESHEET WITHOUT PARTITION PLATE - HOOP STRESS (S_y)

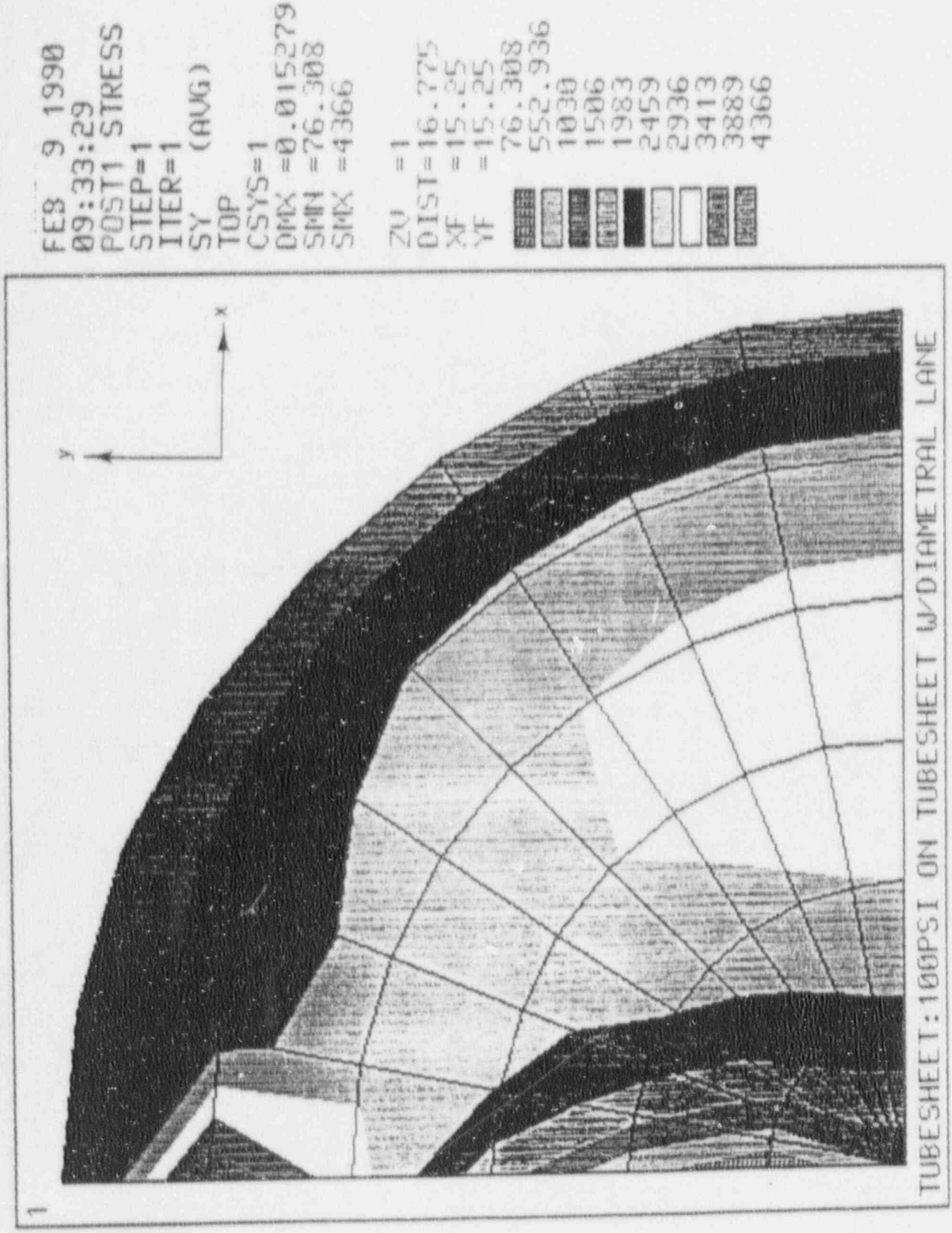

FIGURE 5.13 TUBESHEET WITH PARTITION PLATE - HOOP STRESS (S_y)

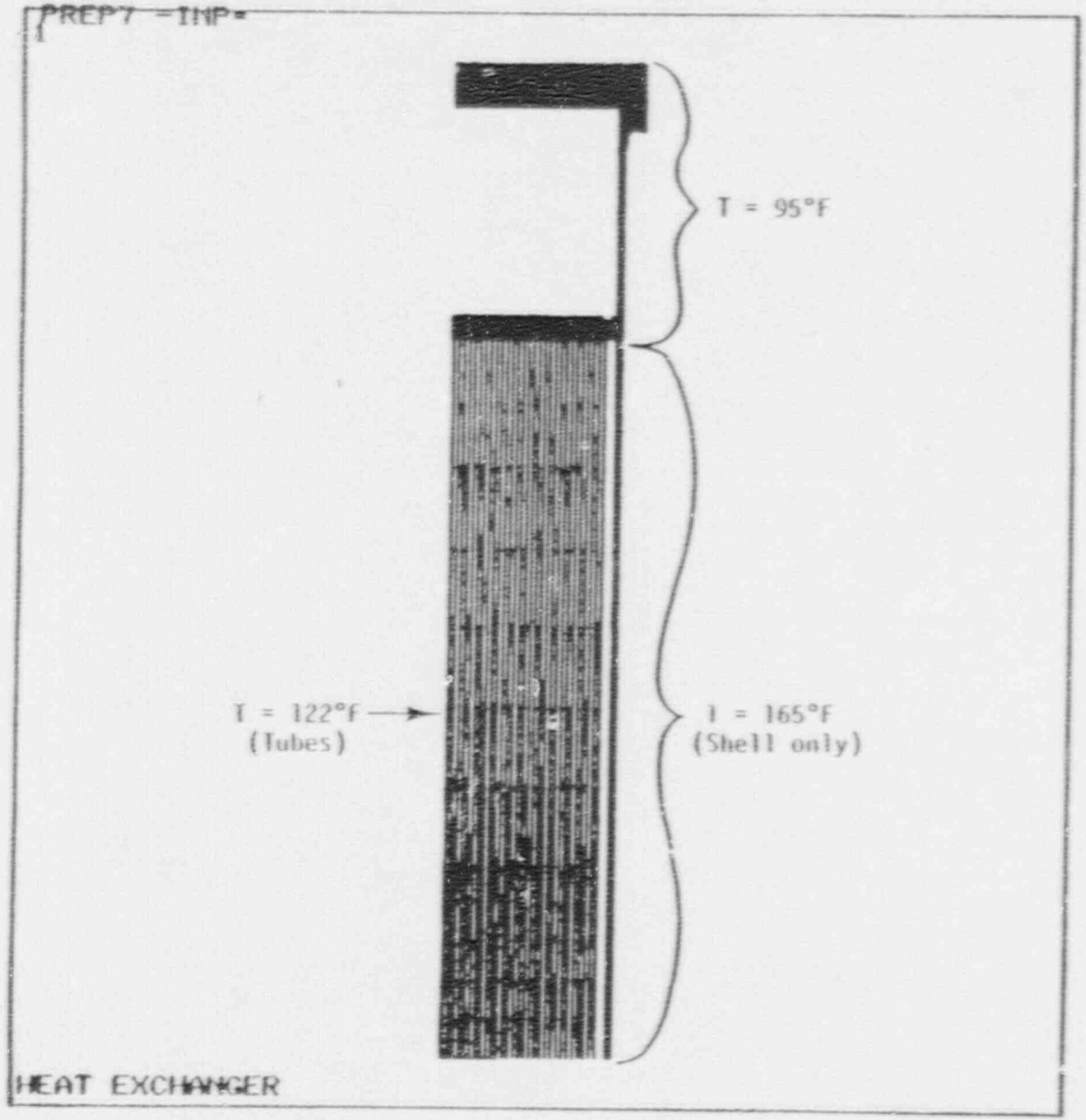

FIGURE 5 14 STEADY-STATE OPERATING TEMPERATURES

NON PROPRIETARY VERSION

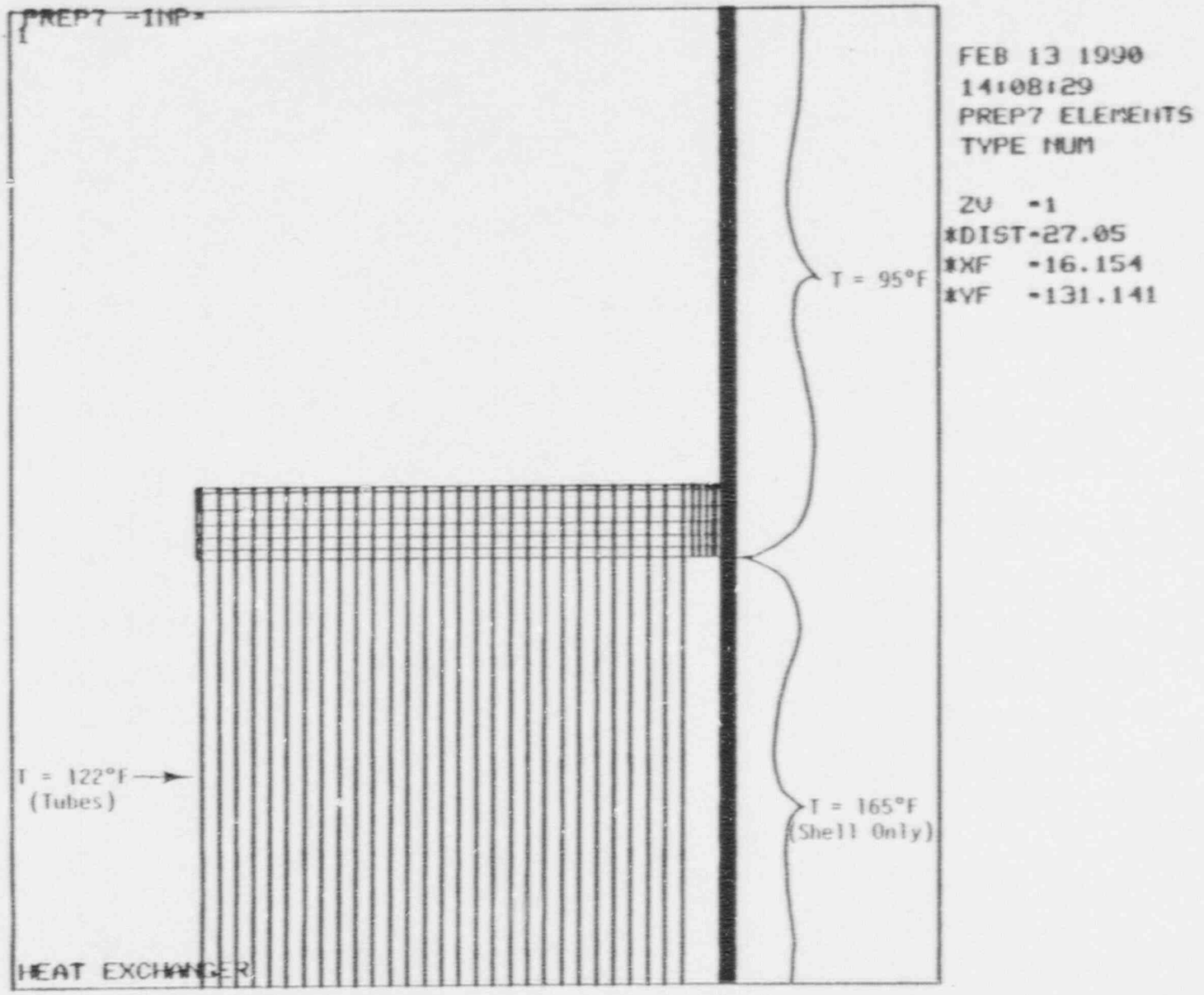

FIGURE 5.15 STEADY-STATE OPERATING TEMPERATURES

NON PROPRIETARY VERSION

6.0 3-DIMENSIONAL ELEMENT ANALYSIS

6.1 Development of 3-D Finite Element Model

A three-dimensional finite element model of the region of interest is shown in Figures 6.1 to 6.5. This model uses isoparametric solid elements to represent the quarter symmetry region. Cut boundary nodes on the 3-D model have the displacements from the 2-D model applied at their common locations (cut boundary locations). See Figure 6.3.

General material properties for the components included in the 3-D finite element model are given in Section 3.2 of this report. Material properties utilized for the 3-D finite element analysis are summarized in Appendix B.1.

6.2 Base Case Loads

The 3-D finite element model is analyzed for the same base case loads that the 2-D finite element model is analyzed for. For the shell side pressure case, internal pressure is applied to the inside of the nozzle as well as the shell. A blowoff load is applied to the nozzle safe end as an outward acting pressure with a magnitude of 629.2 psi

For the tube side pressure case, pressure is applied only to the tubesheet rim on the tube side. The steady-state thermal case has the same temperatures applied as the 2-D model except for the addition of the support bracket temperature of 70°F (acting as a cooling fin). The thermal gradients can be seen in Figure 6.6.

For all cases, displacement boundary conditions include symmetry constraints at $x = 0$ and $z = 0$ planes by fixing all nodes on these two planes in the θ-direction (see Figure 6.4). Also, bolt attachments are simulated at their corresponding locations in the vertical support bracket by fixing nodes at

these locations in the x and z directions (see Figure 6.5). Displacements from the 2-D finite element model for each base load case are then applied to the 3-D finite element model at the cut boundary locations (see Figure 6.3).

6.3 Operational Loads

The operational loads analyzed in the 3-D finite element analysis are the same as those analyzed in the 2-D finite element analysis. The steady-state operating load includes tube side pressure, shell side pressure and steady-state operating temperatures along with steady-state operation displacements from the 2-D model. The preload effects are accounted for in the displacements from the 2-D model.

The no flow shutdown load includes the assumed worse case shutdown temperature of 51°F. The preload effects are again accounted for in the displacements from the 2-D model.

6.4 3-D Analysis Results

The maximum principal stress due to steady-state operation is 16,711 psi. This value is approximately the same at two places in the vessel. They are the nozzle to shell intersection and the bracket to shell intersection . This stress is the maximum stress the shell side is subjected to.

The principal stresses due to shutdown conditions, at the same locations of the maximum stresses due steady-state operation, are approximately 0 psi. This stress is used as the minimum stress the shell side is subjected to . Therefore, cycling occurs between the maximum and minimum stresses for the fracture mechanics analysis.

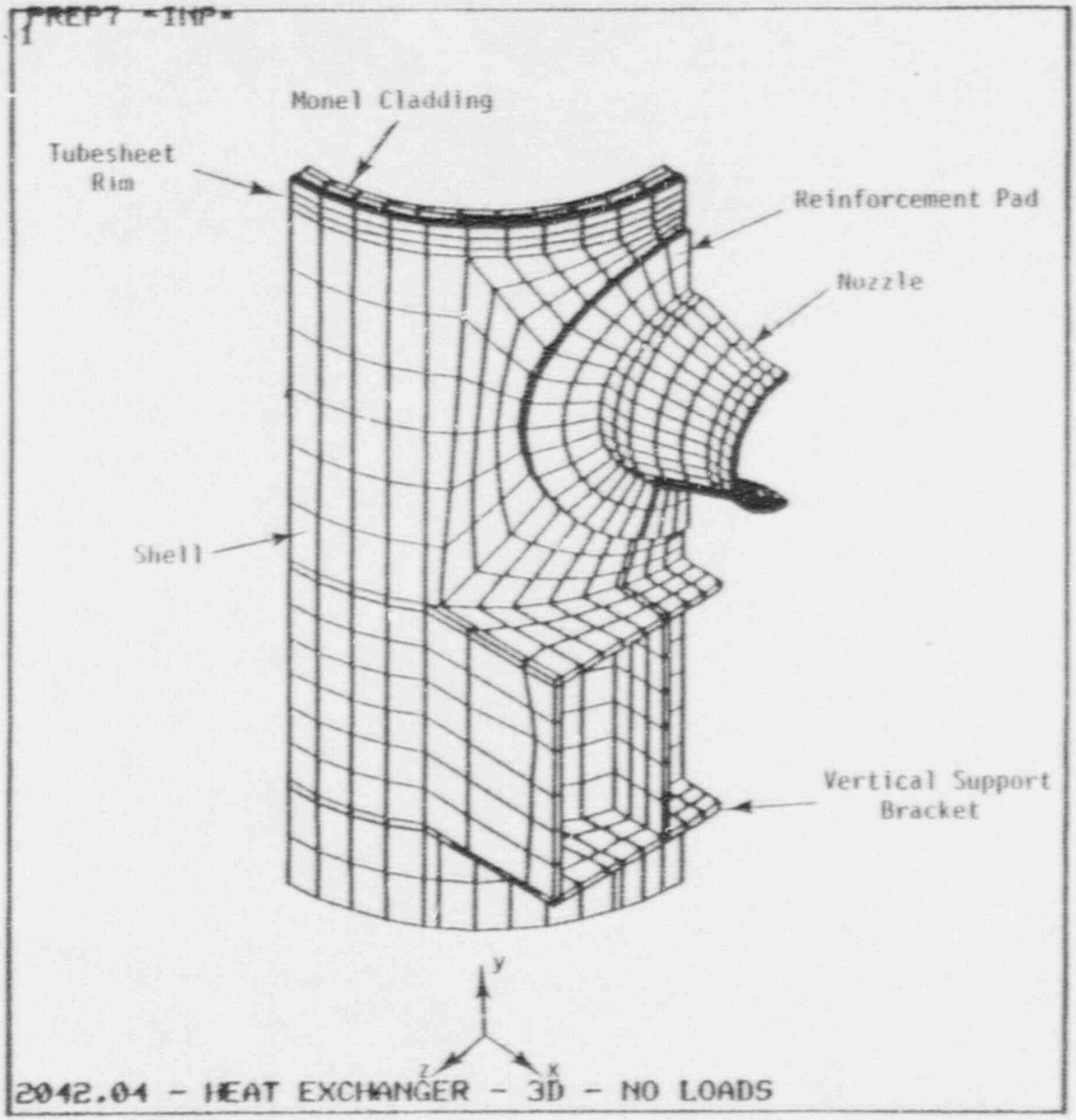

FIGURE 6.1 3-D FINITE ELEMENT MODEL GEOMETRY

NON PROPRIETARY VERSION

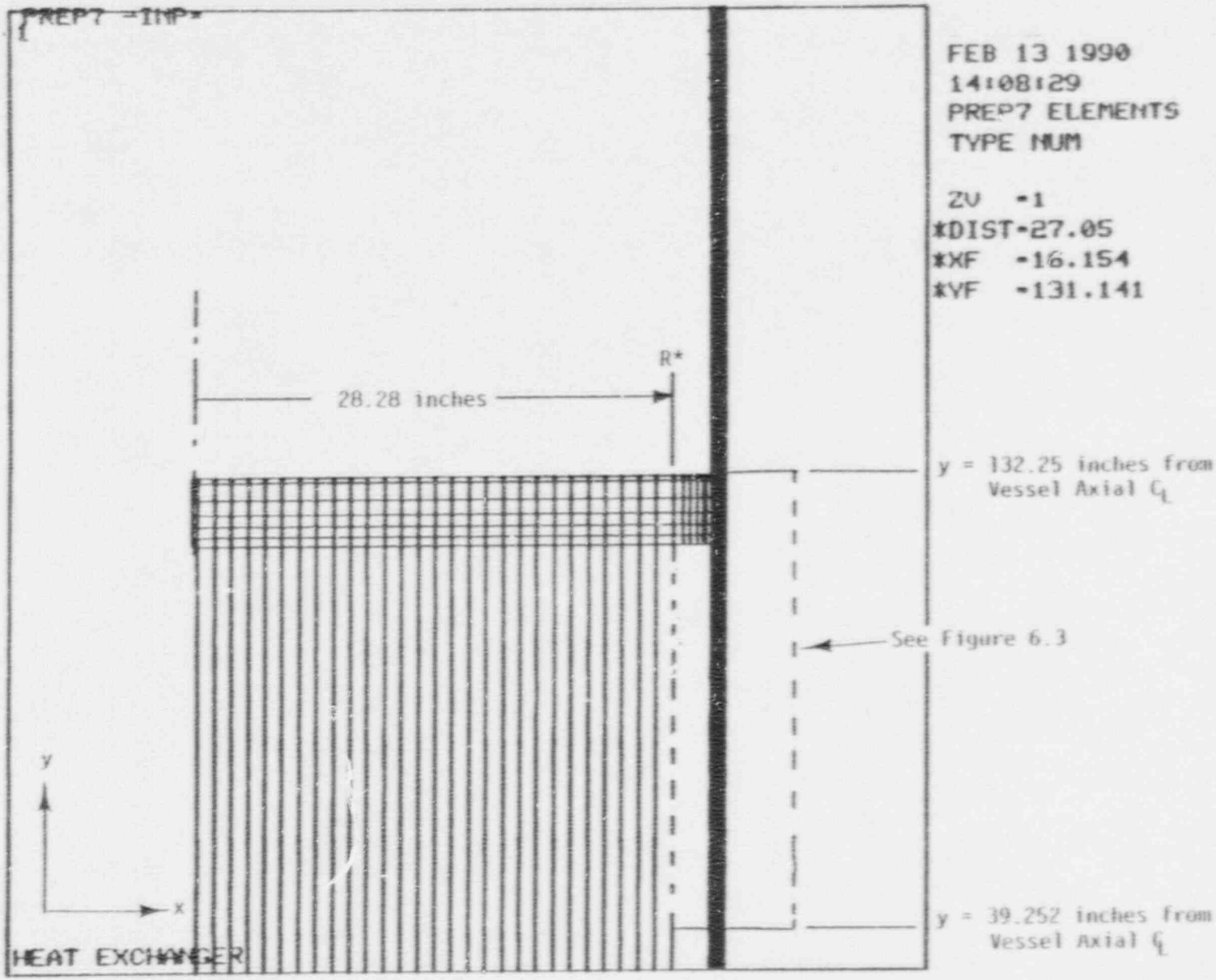

FIGURE 6.2 AXISYMMETRIC CUT BOUNDARIES FOR 3-D FINITE ELEMENT MODEL GEOMETRY

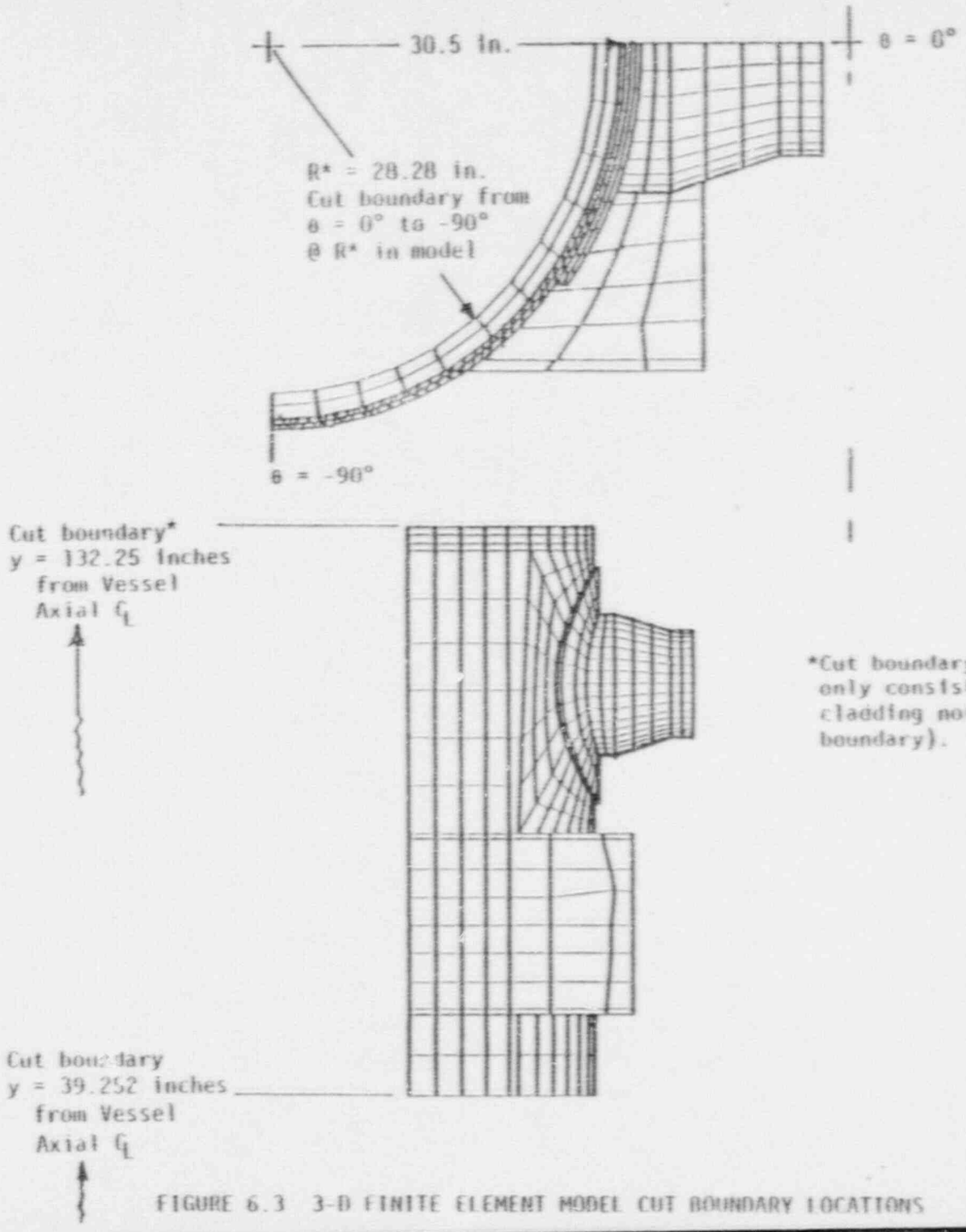

*Cut boundary at this elevation only consists of shell (monel cladding not considered cut boundary).

FIGURE 6.3 3-D FINITE ELEMENT MODEL CUT BOUNDARY LOCATIONS

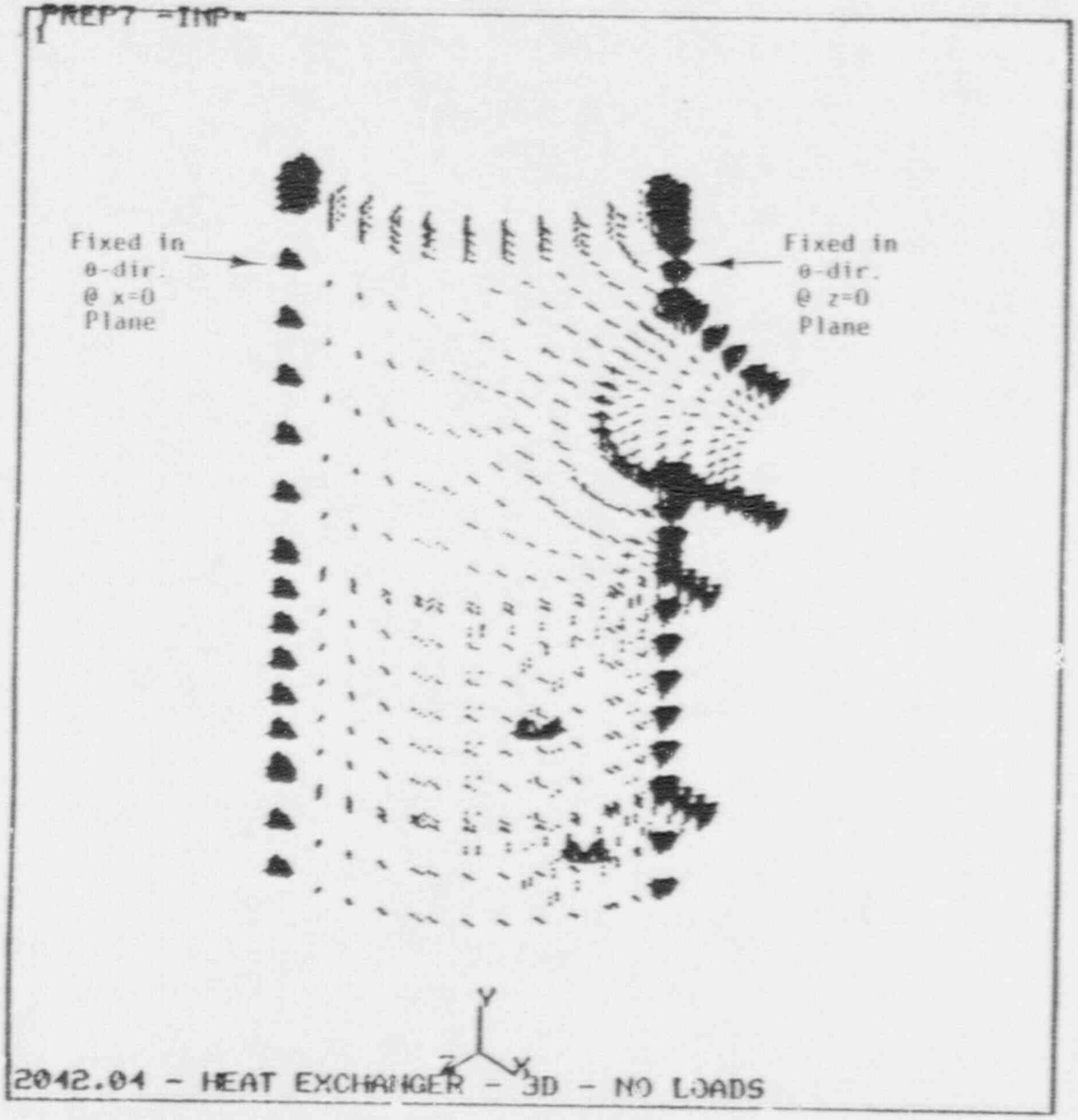

FIGURE 6.4 NODE PLOT OF DISPLACEMENT BOUNDARY CONDITION

NON PROPRIETARY VERSION

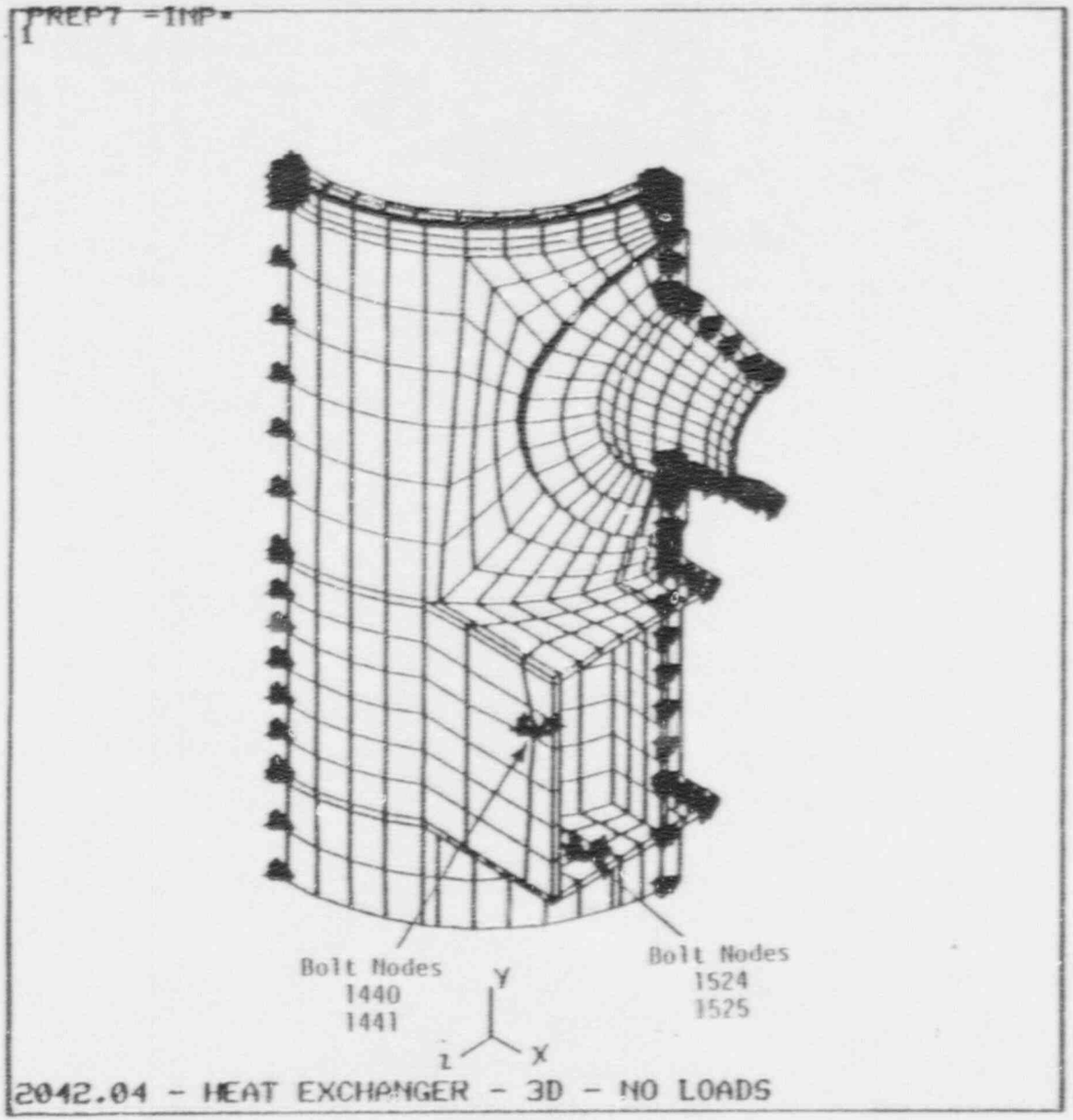

FIGURE 6.5 BOLTED BRACKET CONNECTION LOCATIONS

NON PROPRIETARY VERSION

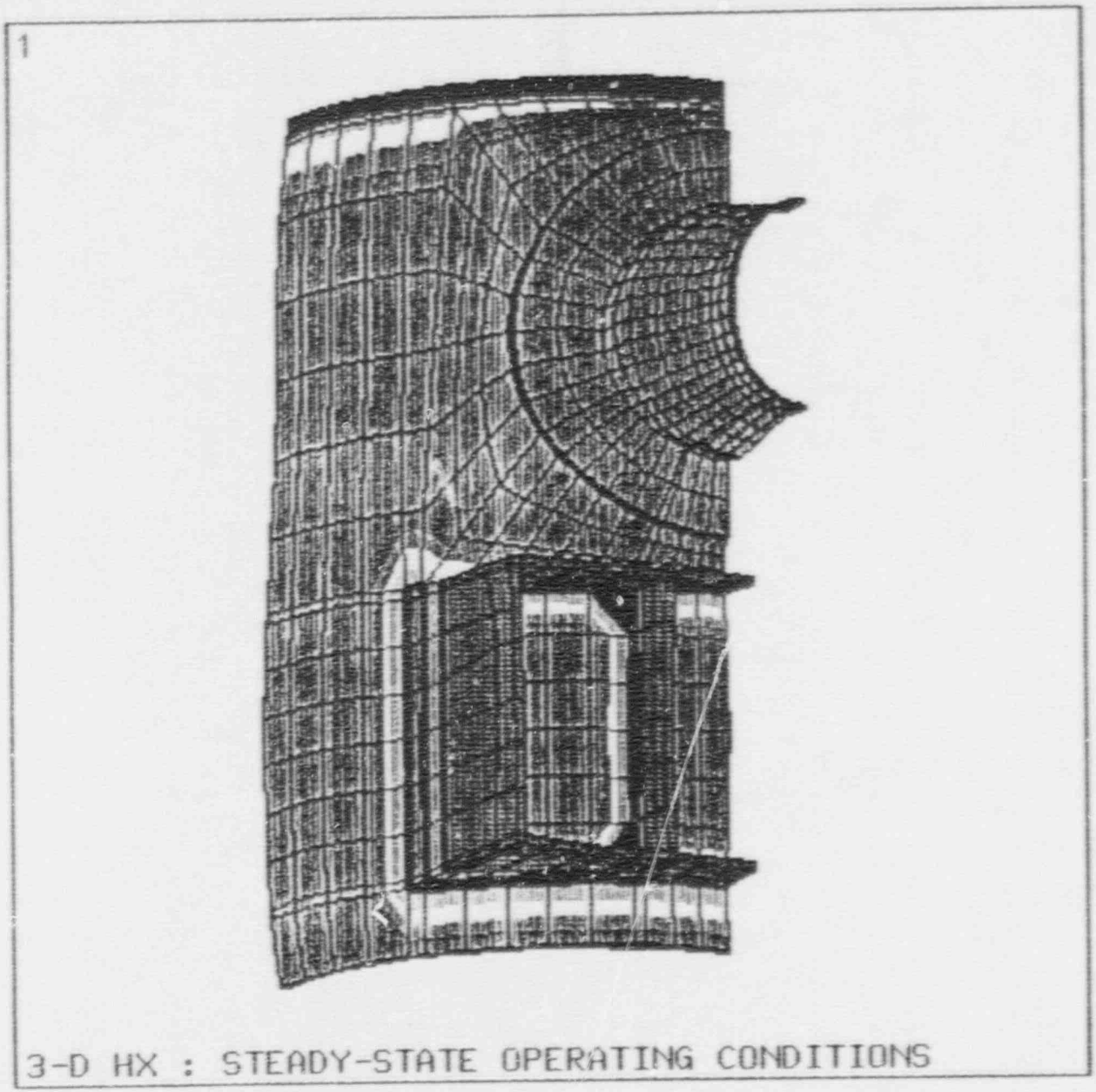

FIGURE 6.6 STEADY-STATE THERMAL GRADIENTS

NON PROPRIETARY VERSION

7.0 FRACTURE MECHANICS ANALYSIS

The stress results from the 3-D finite element analysis are used for the fracture mechanics because they are higher stresses than those from the 2-D finite element analysis. The cyclic stress range from the 3-D analysis is conservatively chosen to be from 0 psi (shutdown conditions) to 16,700 psi (steady-state operation).

The material toughness, K_{IC}, of 76 ksi $\sqrt{in.}$ used to calculate the critical crack size at which failure would occur, A_{cr}, was obtained from an approximate K_{IC} vs. temperature plot using dynamic A-212B data taken from . Because only two data points are given, it is reasonable to assume these two points define the upper and lower shelf values of the ductile-brittle transition region . To obtain temperature adjusted data, the two data points were shifted to the right by 17°F. This moves the upper shelf datum point at 60°F to the lowest allowable service temperature, 77°F, . The straight line connecting the two adjusted transition boundary points was used to determine the conservative estimate of K_{IC} = 76 ksi $\sqrt{in.}$ at 51°F, the minimum expected vessel temperature.

The two data points could also have been shifted to the right by 37°F to bring the NDT, defined below, to the lowest allowable service temperature. This was not done because the low cyclic strain rates between shutdown and steady-state operation of LPCI-HX are consistent with the use of K_{IC} fracture toughness values. Estimating K_{IC} using dynamic K_{ID} data embodies substantial conservatism since the temperature shift between K_{IC} and K_{ID} is approximately 158°F, via the Barsom shift . This shift is calculated based upon the yield stress of 38 ksi for A-212B.

To relate the material toughness to the nil ductility temperature (NDT) of 40°F , K_{IC} was calculated . The straight line between this value, 57 ksi $\sqrt{in.}$ and the adjusted upper bound of the transition region, 98 ksi $\sqrt{in.}$ could also be used to conservatively evaluate K_{IC} at 51°F as indicated . It was judged that this K_{IC} value of 69 ksi $\sqrt{in.}$ is unnecessarily conservative, so the 76 ksi $\sqrt{in.}$ was used in the fracture mechanics evaluation. However, it is apparent from the extremely long calculated fatigue life discussed below that the 69 ksi $\sqrt{in.}$ material toughness would also have been adequate.

For the calculated maximum stress from the 3-D analyses, 16.7 ksi, the critical crack size at which failure would occur is 5.25 inches . Using the maximum stress range (0.0 - 16.7 ksi) and the crack growth rate equation , the number of cycles, N, required for various assumed initial crack sizes, A_i, to grow to the critical size, A_{cr}, is calculated .

The results, based upon an initial crack size of .010 inch (chosen as the maximum crack size that could go undetected by inspection of the unit at the time of its construction) and a cold HX shutdown temperature of 51°F, show that the number of cycles that would be required to propagate a crack of this size to the critical crack size is approximately 1.5×10^6. Since the critical crack size is greater than the wall thickness an additional calculation was performed which showed that the number of cycles that would be required to propagate the initial crack through the wall is approximately 1.4×10^6.

. From t. 9 results it can be seen that the crack should begin to leak approximately 96,000 cycles before it would fail.

Based solely from this fracture mechanics analysis and a system startup and shutdown cycle occurring on an average of once a month, the acceptable number of cycles is far beyond any anticipated service life of the LPCI-HX as well as several orders of magnitude beyond the maximum conceivable plant li e including life extension. Therefore, it is concluded that the fracture toughness of the shell side of the LPCI-HX is more than adequate.

8.0 REFERENCES

8.0 REFERENCES (Con't)

APPENDIX A

AXISYMMETRIC TUBESHEET FINITE ELEMENT MODEL APPENDIX

Appendix A.1

Finite Element Model Material Properties

Appendix A.2

Adjusted Material Properties for Stud Hole Regions

Appendix A.3

Tubesheet and Tube Data

Appendix A.4

Stud Bolt Properties

Appendix A.5

Calculation of Closure Stud Preload

Appendix A.6

Calculation of Tube Temperature

Appendix A.7

Axisymmetric Analysis Results

APPENDIX B

3-D FINITE ELEMENT MODEL APPENDIX

Appendix B.1

3-D Finite Element Model Material Properties

Appendix B.2

Calculation of Blowoff Pressure

Appendix B.3

3-D Analysis Results

APPENDIX C

FRACTURE MECHANICS ANALYSIS APPENDIX

Attachment A

Fracture Toughness Evaluation of the

Shell Side of the LPCI Heat Exchanger for

Dresden Station Unit 2

(Propietary Report - Report No. 2042.04-400-001-00)